

Peer review status:

This is a non-peer-reviewed preprint submitted to EarthArXiv.

Lagged impacts of groundwater pumping on streamflow due to stream drying: Incorporation into analytical streamflow depletion estimation methods

Authors: Sam Zipper^{a,b,*}, Ian Gambill^a, Monty Schmitt^c, Claire Kouba^d, Leland Scantlebury^e, Thomas Harter^f, Nicholas P. Murphy^c

Affiliations:

a. Kansas Geological Survey, University of Kansas, 1930 Constant Ave, Lawrence KS 66044, USA

b. Department of Geology, University of Kansas, 1414 Naismith Drive, Lawrence KS 66045, USA

* Corresponding author: samzipper@ku.edu

c. The Nature Conservancy, 830 S Street, Sacramento CA 95811

d. Yale University, School of the Environment, 195 Prospect Street, New Haven, CT 06511, USA

e. Hydrologic Sciences Graduate Group, University of California, Davis, 1 Shields Ave, Davis CA 95616

f. Department of Land, Air and Water Resources, University of California, Davis, 1 Shields Ave, Davis CA 95616

ORCID + email:

SZ: 0000-0002-8735-5757, samzipper@ku.edu

IG: 0000-0001-7653-4066, ian.gambill@ku.edu

MS: N/A, monty.schmitt@tnc.org

CK: 0000-0002-6381-8315, claire.kouba@yale.edu

LS: 0000-0002-6770-063X, lscantle@ucdavis.edu

TH: 0000-0001-8526-3843, thharter@ucdavis.edu

NM: 0000-0001-8442-0747, nicholas.murphy@tnc.org

Highlights

- Analytical depletion functions (ADFs) estimate streamflow depletion caused by pumping
- ADFs incorporating stream drying had strong agreement with observed streamflow
- Stream drying shifts timing of streamflow depletion due to hydrologic disconnection
- Modeling stream drying requires accurate estimates of non-depleted streamflow
- Strong ADF performance suggests potential use as a low-cost decision-support tool

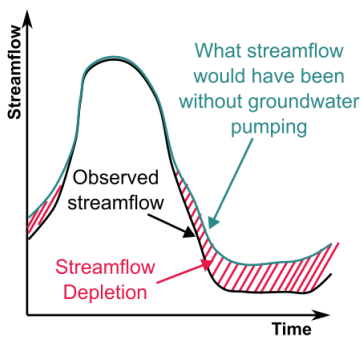
Non-peer-reviewed manuscript submitted to Journal of Hydrology, June 2025

40 **Abstract**

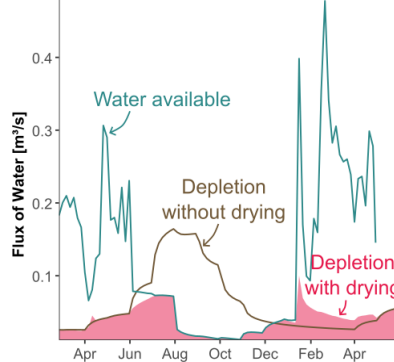
41 Water management often requires accounting for reductions in streamflow caused by
42 groundwater pumping ('streamflow depletion'). Since streamflow depletion cannot be quantified
43 from observational data, it is typically modeled. Analytical depletion functions (ADFs) are a
44 low-cost, low-complexity approach for estimating streamflow depletion with utility for decision
45 support, but ADFs adopt several simplifying assumptions, including an infinite supply of water
46 within the stream. Here, we develop an approach to incorporate stream drying into ADFs to
47 improve their estimation of streamflow and streamflow depletion. Using Scott Valley
48 (California) as an example, we compare ADF results to observed streamflow data and the Scott
49 Valley Integrated Hydrologic Model (SVIHM), a process-based numerical model of the domain.
50 ADFs incorporating stream drying simulate strong agreement with observed streamflow and
51 SVIHM results. Critically, ADFs with drying can simulate a temporal shift in streamflow
52 depletion that occurs when summer stream drying causes stream network disconnections and a
53 substantial fraction of streamflow depletion is lagged until the fall/winter, when the stream
54 network rewets. Estimates of what streamflow would have been without groundwater pumping
55 are required to incorporate stream drying into ADFs, and we evaluate the ability of a statewide
56 statistical model of unimpaired monthly streamflow (the California Natural Flows Database
57 [CNFD]) to meet this need. ADFs using CNFD data simulate appropriate temporal dynamics but
58 overestimate streamflow, suggesting that regional unimpaired flow estimates combined with
59 local bias-correction could provide a mechanism to apply ADFs in watersheds without local
60 numerical models.

61
62 **Graphical Abstract**

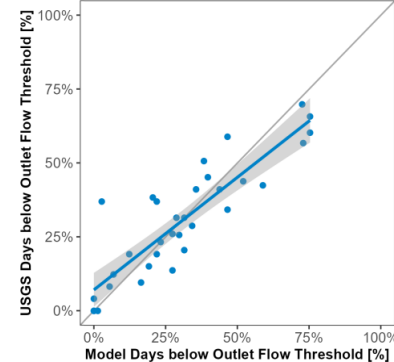
Analytical depletion functions (ADFs) are simple tools to estimate streamflow depletion caused by groundwater pumping



We show that stream drying changes the timing of streamflow depletion and simulate this using ADFs.



ADF simulated streamflow closely matches stream gauging data and output from a local integrated hydrologic model.



63
64

65 **Keywords:** streamflow depletion, groundwater pumping, non-perennial streams, groundwater-
66 surface water interactions, California, SGMA, integrated water resources management

67

68 **1. Introduction**

69 While surface water and groundwater resources have historically been managed and
70 regulated separately (Gage & Milman, 2020), in many settings they are a single interconnected
71 resource (Winter et al., 1998). Reductions in streamflow caused by groundwater pumping,
72 known as ‘streamflow depletion’ (Barlow et al., 2018; Barlow & Leake, 2012), are a primary
73 mechanism by which groundwater use can affect surface water resources and groundwater-
74 dependent ecosystems (Rohde et al., 2017). In recent decades, water management frameworks
75 have emerged which require quantifying and accounting for interconnections between
76 groundwater and surface water, such as streamflow depletion, when developing water
77 management plans. For example, the European Water Framework Directive and the Australian
78 National Water Initiative both specify that groundwater use cannot impair interconnected surface
79 water resources (Kallis & Butler, 2001; Rohde et al., 2017; Ross, 2018; Vázquez-Suñé et al.,
80 2006). In the United States, California’s Sustainable Groundwater Management Act (SGMA)
81 was passed in 2014, requiring specific priority groundwater subbasins to achieve groundwater
82 sustainability by 2040. SGMA defines sustainability as long-term groundwater management
83 which prevents significant and unreasonable undesirable results, including the depletion of
84 interconnected surface waters (Harter, 2020; Leahy, 2016; Owen et al., 2019). Under SGMA,
85 groundwater managers are expected to estimate the location, timing, and quantity of
86 interconnected streamflow depletion occurring due to groundwater pumping (California
87 Department of Water Resources, 2024).

88 Quantifying streamflow depletion is challenging because pumping impacts are frequently
89 obscured by other causes of variability such as weather/precipitation dynamics, surface water
90 impoundments/diversions, and lags between groundwater pumping and streamflow impacts
91 (Barlow & Leake, 2012). Streamflow depletion can be directly measured using observational
92 data at the reach scale over short timescales (Flores et al., 2020; Hunt et al., 2001; Kollet &
93 Zlotnik, 2003; Malama et al., 2024; Nyholm et al., 2002). However, due to the intensity of data
94 requirements, streamflow depletion cannot be quantified using solely observational data at
95 management-relevant scales such as aquifers or watersheds, and is instead modeled using a
96 variety of approaches (Zipper et al., 2022a). Numerical models, such as MODFLOW, MIKE-
97 SHE, and HydroGeoSphere, simulate stores and fluxes of water in groundwater and surface
98 water systems using physical governing equations and can be calibrated to local data such as
99 streamflow and groundwater levels (Falke et al., 2011; Fienen et al., 2018; RRCA, 2003; Tolley
100 et al., 2019). These models are generally considered the most reliable tools for assessing
101 streamflow depletion due to their process-based foundation and opportunity for site-specific
102 calibration. Due to their complexity they also have high development costs in terms of data,
103 effort, and expertise (Barlow & Leake, 2012; Zipper et al., 2022a).

104 Analytical depletion functions (ADFs) have been proposed as a low-cost and scalable
105 approach for estimating streamflow depletion (Zipper et al., 2019). ADFs are based on analytical
106 models for streamflow depletion, which mathematically simplify physical governing equations
107 by adopting assumptions, commonly including a well pumping in a homogeneous subsurface
108 connected to a single stream partially or fully penetrating into the aquifer system (Glover &

109 Balmer, 1954; Hantush, 1965; Huang et al., 2018; Hunt, 1999). ADFs extend analytical models
110 by using empirical approaches to address some of these assumptions, for example by identifying
111 multiple potentially affected stream segments by each well and distributing depletion among
112 stream segments using geometric approaches known as depletion apportionment equations
113 (Zipper et al., 2018; additional details in Section 2). However, one analytical simplification that
114 has not been addressed by ADFs is the assumption of an infinite supply of water in the stream.
115 Non-perennial (intermittent or ephemeral) streams are common, estimated to make up more the
116 half the global river network (Messenger et al., 2021), and are becoming increasingly widespread
117 due to climate change and human activities (Sauquet et al., 2021; Trambly et al., 2021; Zipper
118 et al., 2021a). Furthermore, in settings where pumping is a substantial fraction of the water
119 balance, streamflow depletion itself can lead to reductions in stream storage and stream drying
120 (Datry et al., 2022; Malama et al., 2024; Zipper et al., 2022b), which violates the assumption of
121 infinite water.

122 To advance integrated groundwater-surface water decision-making capabilities in
123 watersheds affected by groundwater pumping, this study asks, how does the incorporation of
124 stream drying and the downstream accumulation of streamflow depletion affect the ability of
125 ADFs to simulate spatial and temporal patterns of streamflow and streamflow depletion? To
126 accomplish this, we compare ADF simulations of streamflow and streamflow depletion to
127 observed streamflow data and output from the process-based Scott Valley Integrated Hydrologic
128 Model (SVIHM; Foglia et al., 2013, 2018; Tolley et al., 2019) in the Scott River Valley
129 (California, USA). We develop a novel and simple water budget-based approach to represent
130 stream drying that accounts for temporal shifts in streamflow depletion caused by stream
131 network drying and is able to propagate both pumping and drying impacts through the river
132 network. We also demonstrate how a regional statistical model of unimpaired streamflow
133 provides a potential approach for ADF implementation in ungauged and unmodeled watersheds.

134

135 **2. Analytical depletion function (ADF) theory and development**

136 Analytical depletion functions have three primary steps to estimate the impacts of
137 groundwater pumping on streamflow (Figure 1a), which are described in Zipper et al. (2019).
138 First, ‘stream proximity criteria’ are used to identify the stream segments that could be affected
139 by a well based on stream network geometry (Zipper et al., 2019). Second, ‘depletion
140 apportionment equations’ distribute depletion among the affected segments using stream network
141 geometry (Huggins et al., 2018; Reeves et al., 2009; Zipper et al., 2018). Third, the streamflow
142 depletion is calculated separately for each affected stream segment using an analytical model
143 (Glover & Balmer, 1954; Hantush, 1965; Hunt, 1999) and scaled based on the apportioned
144 depletion from step two. The resulting output is a three-dimensional streamflow depletion
145 response matrix (White et al., 2021) that quantifies the individual response of each stream
146 segment to each pumping well at each simulated timestep. The impacts of multiple wells on a
147 given segment are assumed to be linearly additive. The specific approaches used for each of
148 these steps in this study are described in Section 3.4.

149 Past work has evaluated multiple different approaches for each of these steps via
150 comparison to numerical models in a variety of hydrogeological settings including coastal
151 California, coastal and interior British Columbia, and the U.S. High Plains aquifer region (Li et
152 al., 2020; Zipper et al., 2018, 2019, 2021b). This work has shown that ADF and numerical model
153 simulations largely agree for several aspects of pumping impacts on stream networks, including
154 identifying the segment with the greatest streamflow depletion by a given well, the magnitude of
155 depletion in that segment, and the overall spatial distribution and magnitude of depletion across
156 all affected stream segments (Li et al., 2022; Zipper et al., 2019). However, this past work has
157 only used intermodel comparisons for accuracy assessment and has not included any direct
158 comparison to observational data, such as streamflow from gauging stations. Additionally, these
159 evaluations focused on segment-resolution changes in stream-aquifer flux rather than the
160 accumulated streamflow depletion within the stream network and do not account for limited
161 surface water supply (stream drying).

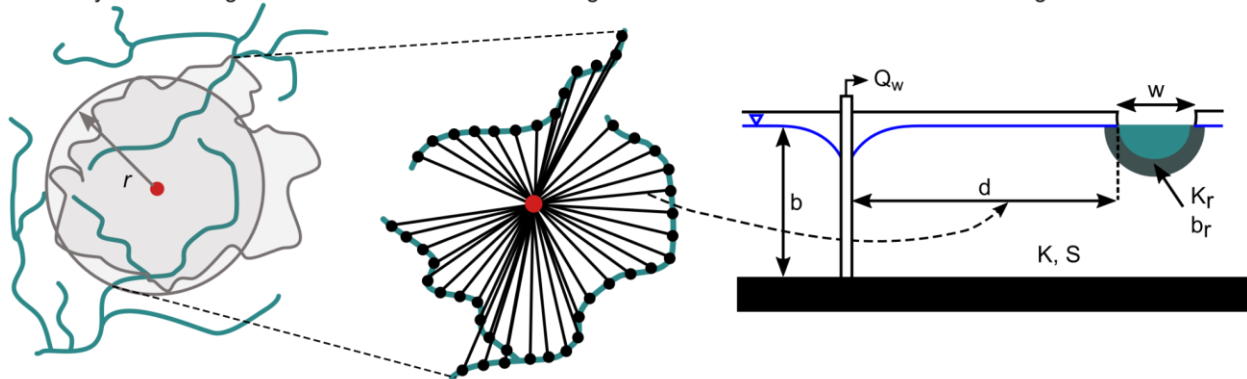
162 In this study, we advance the development of ADFs through two interlinked process
163 representations: (i) the routing of streamflow and streamflow depletion through the stream
164 network, and (ii) stream drying, which leads to a redistribution of depletion in time and space
165 (Figure 1b). To accomplish this, we defined the stream network as a directed graph, with each
166 stream segment represented by a node. To account for potential drying at a given segment, we
167 incorporated an estimate of the streamflow that would have occurred in a segment if there were
168 no groundwater irrigation, which we refer to as “water available”.

169 Combining the two steps, for each timestep, the resulting streamflow is calculated as the
170 difference between water available and ADF depletion if and only if the calculated cumulative
171 depletion by the ADFs in that segment and in upstream segments is less than the water available.
172 If the depletion exceeds the amount of water available, the depletion is assumed to dry the stream
173 and any calculated depletion in excess of water available is “banked” for a later timestep in the
174 same stream segment.

175 Once additional water is available in the stream, banked streamflow depletion is added to
176 the calculated depletion for each timestep, but only up to the water available for depletion in the
177 segment. Thus, a timeseries of redistributed depletion is generated. For each simulated timestep,
178 streamflow and streamflow depletion are calculated starting from headwater segments and
179 moving downstream through the stream network so that any temporal redistributions of
180 streamflow depletion are propagated to downstream segments. Details for how these steps are
181 specifically implemented for our study domain are provided in Section 3.

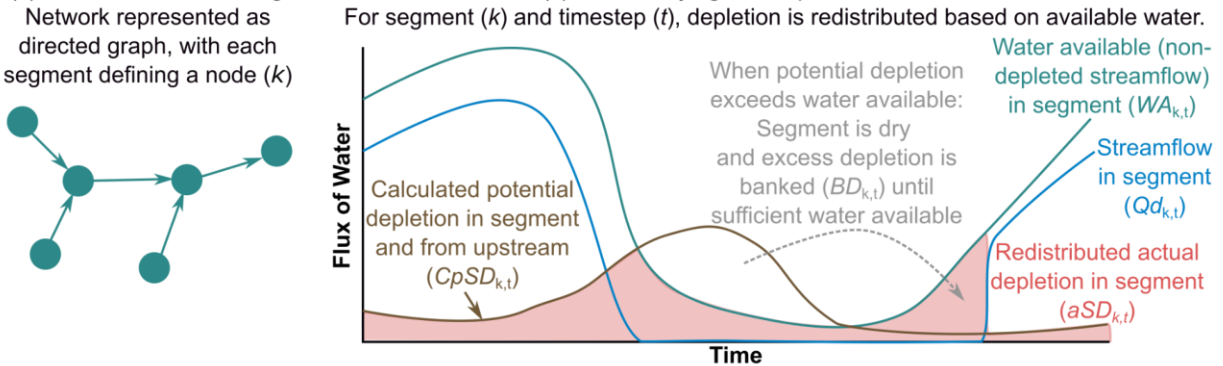
(a) Analytical depletion function workflow

- (1) *Stream Proximity Criteria: Adjacent + Expanding*
Identify affected segments
- (2) *Depletion Apportionment: Web Squared*
Calculate fractional depletion for each segment
- (3) *Analytical Model: Hunt (1999)*
Calculate volumetric depletion for each segment



(b) Depletion routing and stream drying

- (4) *Stream network routing*
Network represented as directed graph, with each segment defining a node (k)
- (5) *Stream drying and depletion redistribution*



Streamflow ($Q_{d,k,t}$) calculated as water available ($WA_{k,t}$) minus actual depletion ($aSD_{k,t}$).

Figure 1. (a) Overview of analytical depletion functions (ADFs) and (b) methods for incorporating depletion routing and stream drying into ADFs. The specific equations and variables in panel a(3) are defined in Section 3.4.

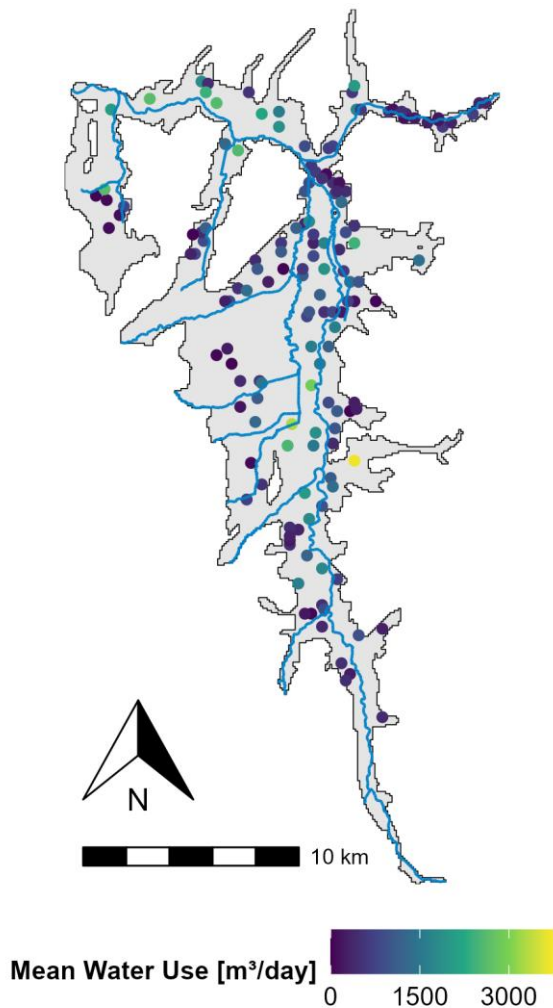
3. Methods

In this study, we develop and test ADFs including stream drying and depletion routing via comparison to stream gauging data and a process-based numerical hydrologic model (SVIHM) in the Scott Valley region of California.

3.1 Study domain: Scott Valley, California

Nestled in the Siskiyou mountains in Northern California, Scott Valley is a Mediterranean-climate montane valley 800 m above sea level and approximately 200 km² in area (Tolley et al., 2019). The Scott River runs north through the valley (Figure 2), draining an area approximately 2100 km² and eventually flowing into the Klamath River. Land use in the flat portions of the valley floor is almost entirely agricultural, with alfalfa and pasture land comprising the largest proportions, while the surrounding uplands are largely managed as part of Klamath National Forest. Agricultural irrigation is the primary use of water, as the 500 mm of average precipitation that occurs in the valley falls between October-May, while the primary growing season is April-September.

200 The Scott River provides habitat to a variety of native aquatic fauna, including Chinook
201 salmon and threatened coho salmon. Quantifying streamflow depletion therefore is critical to
202 effective ecohydrological management. In an attempt to protect these aquatic populations,
203 minimum flow requirements (details in Section 4.3.1) have been suggested for the Scott River at
204 the Fort Jones gauge operated by the U.S. Geological Survey (USGS; gauge 11519500). The
205 Scott River at Fort Jones gauge is located immediately downstream of the closed intermontane
206 valley floor (41.64069017°N, 123.015037°W) at the top of a narrower bedrock canyon, and has
207 streamflow records dating back to 1941. The valley floor is underlain by an aquifer made up of
208 fluvial and alluvial deposits of gravels, sands, silts and clays that form a productive aquifer
209 greater than 120 m thick in places (Mack, 1958), underlain by very low permeability,
210 heterogeneous fractured bedrock. This aquifer system is strongly connected to the river system
211 and stream-aquifer exchange is highly spatially and temporally heterogeneous (Tolley et al.,
212 2019).



213
214 Figure 2. Scott Valley study domain. The grey shaded area is the active SVIHM model domain. Blue lines show the
215 stream network, with the watershed outlet in the northwest corner of the domain. Pumping wells are colored by their
216 average water use over the period of comparison.
217

218 3.2 Scott Valley Integrated Hydrologic Model (SVIHM)

219 SVIHM consists of three models run sequentially: an upper watershed tributary
220 streamflow regression model, a soil-crop-water balance (agricultural water demand) model, and
221 a numerical groundwater flow model using MODFLOW-NWT (Niswonger et al., 2011). The
222 streamflow regression model predicts inflows into the topographically flat portion of Scott
223 Valley overlying the aquifer system using statistical relationships estimated between the tributary
224 gauges (dependent variable) and the Fort Jones gauge (independent variable). The soil-crop-
225 water balance model estimates surface water and groundwater abstraction using a crop-
226 coefficient based ET estimation and field-scale information about crops, soils, irrigation systems,
227 their efficiency, and water sources (Foglia et al., 2013; Tolley et al., 2019). Recharge to the
228 underlying aquifer system is estimated for each field using a tipping-bucket approach; the
229 method and underlying equations are fully documented in Tolley et al. (2019). The MODFLOW-
230 NWT model simulates the coupled groundwater-surface water system. The model consists of 2
231 layers, 440 rows and 210 columns (19,869 and 14,054 active nodes in layers 1 and 2,
232 respectively), each 100m x 100m in size, and aquifer properties vary spatially via nine
233 contiguous, homogenous hydrogeologic zones (Tolley et al., 2019). The model has monthly
234 stress periods, daily time steps, and uses tab files to input the tributary inflows into the valley on
235 a daily basis.

236 SVIHM has been used as a decision-support tool in Scott Valley for over a decade
237 (Foglia et al., 2013, 2018; Kouba & Harter, 2024; Siskiyou County Water Conservation and
238 Flood Control District, 2021; Tolley et al., 2019). Agricultural water use data are not available in
239 the region, and thus the model serves an important purpose in estimating the valley water use and
240 water balance. Additionally, SVIHM facilitates a wide variety of scenarios to be tested, e.g.,
241 removal/addition of pumping wells, land use changes, irrigation method changes, groundwater
242 and surface water curtailments, droughts, etc. The specific SVIHM scenarios used in this study
243 are described in Section 3.4.3.

244 3.3 California Natural Flows Database (CNFD)

245 The California Natural Flows Database (CNFD) is the result of a modeling approach
246 developed in partnership between the California Environmental Flows Framework
247 (<https://ceff.ucdavis.edu/>) technical team and the U.S. Geological Survey (USGS) that uses
248 machine learning models to predict monthly unimpaired flows across the state of California.
249 Unimpaired flows are a key water resource management consideration, particularly for the
250 conservation of aquatic ecosystems. Modeling the natural flow regime allows for an increased
251 understanding of existing alteration across surface water systems. Zimmerman et al. (2018)
252 identified 250 reference stream gages with minimal flow alteration and divided them into three
253 regions based on climate and hydrologic conditions. Using observed monthly flows, climate and
254 run-off variables, and fixed physical watershed characteristics, they developed random forest
255 statistical models for each region. These random forest models were then applied to predict flows
256 for all streams in the state, estimating natural flow values from 1950 to 2015 at stream segment

257 resolution (based on the resolution of the U.S. National Hydrography Dataset [NHD]), along
258 with the range of uncertainty (Zimmerman et al., 2018).

259 Predictive accuracy of the model was assessed by comparing predicted monthly
260 minimum, mean, and maximum flows to observed flows at randomly selected reference stream
261 gages believed to have natural flows (locations lacking upstream hydrologic alteration). Average
262 model performance results included the ratio of observed to predicted value of 0.94, an r-squared
263 value of 0.80, a percent bias of -3.30 and a Nash-Sutcliffe Efficiency of 0.75 (Zimmerman et al.,
264 2018). Studies have expanded upon this approach, utilizing modeled natural flows to propose
265 ecologically functional flow metrics for riverine ecosystems statewide (Grantham et al., 2022).
266 The CNFD is continuously updated, and monthly unimpaired flow estimates are available up to
267 the present day (<https://rivers.codefornature.org/>). The specific CNFD data used in this study are
268 described in Section 3.4.3.

269 *3.4 ADF implementation to calculate depletion, streamflow, and drying in Scott Valley*

270 *3.4.1 Calculating potential streamflow depletion from ADFs*

271 ADFs directly calculate the potential streamflow depletion, defined as the amount of
272 streamflow depletion that would occur if the stream had an unlimited supply of water, for each
273 stream segment at each timestep. The primary data sources for ADFs are the hydrostratigraphic
274 parameters of transmissivity and storativity; the locations and pumping schedules for any wells;
275 and the stream network. For our comparison, we used data from SVIHM to parameterize ADFs
276 to maximize input data commensurability for an ‘apples to apples’ comparison. Therefore, our
277 study is intended to understand the differences in simulated streamflow and streamflow depletion
278 that can be attributed to differences in model structure and complexity, rather than differences
279 that may be caused by model input data source or uncertainty (though we do evaluate multiple
280 data sources related to water available). For transmissivity (Tr), we developed gridded maps by
281 multiplying horizontal hydraulic conductivity (K) by aquifer thickness (b) at each SVIHM grid
282 cell. For storativity (S), we summed specific yield (Sy) and the product of specific storage (Ss)
283 and b . Since Sy is substantially larger than $Ss*b$, variation in S is primarily driven by Sy zones
284 within SVIHM. Pumping locations were defined as the center of each SVIHM grid cell with a
285 pumping well, and pumping schedules (Q_w) were obtained from SVIHM as described in Section
286 3.2. The stream network was also defined based on the SVIHM grid. We then summarized
287 hydrostratigraphic input parameters for each potential combination of wells and affected streams
288 using the average Tr and S value for any grid cell along a line connecting each well to the closest
289 point on each stream segment.

290 For ADF implementation, we used the ‘adjacent + expanding’ stream proximity criteria
291 (Figure 1a, step 1), which allows wells to affect streams in any adjacent catchment or within a
292 radial distance that expands with time (details in Zipper et al., 2019). The allowable radial
293 distance at each timestep was based on the 10th percentile of S and 90th percentile of Tr for all
294 well-stream pairs, and is therefore meant to represent an inclusive criteria. For the depletion
295 apportionment equation (Figure 1a, step 2), we used the web-squared approach developed in
296 Zipper et al. (2018) that distributes fractional depletion based on a weighted inverse distance of

297 evenly spaced points along each affected stream segment. The ‘adjacent + expanding’ and ‘web
 298 squared’ approaches have generally been found to provide the best performance in past studies
 299 (Li et al., 2020; Zipper et al., 2018, 2019, 2021b), so we did not conduct additional testing of
 300 alternate stream proximity criteria and depletion apportionment equations in this study.

301 To estimate the amount of streamflow depletion due to pumping in each stream segment
 302 (Figure 1a, step 3), we used the analytical model developed in Hunt (1999) which simulates a
 303 partially-penetrating stream with a streambed layer that impedes flow as a function of its
 304 conductance (λ). For the conductance of the streambed layer, we used the λ values in each
 305 segment as SVIHM. In practice streambed conductance has tremendous fine-scale
 306 spatiotemporal variability (Abimbola et al., 2020b, 2020a; Korus et al., 2018, 2020) and is rarely
 307 known with any confidence (Christensen, 2000), and therefore this parameter is typically
 308 unknown or calibrated. To evaluate the potential impacts of the analytical model selection, we
 309 repeated our analysis using the Glover & Balmer (1954) analytical solution that assumes a fully
 310 penetrating stream with no resistance to flow and therefore does not require λ . We found that
 311 simulated depleted streamflow at the watershed outlet was insensitive to the selection of an
 312 analytical model in this domain (Figure S4), and therefore only results from the Hunt model are
 313 shown throughout the rest of the manuscript. All ADF simulations were done using a five-day
 314 timestep for the period from October 1, 1990 to September 30, 2023 and were implemented
 315 using the streamDepletr package for R (Zipper, 2023).

316 3.4.2 Incorporating depletion routing and stream drying

317 The ADF as described in Section 3.4.1 and shown in Figure 1a calculates the potential
 318 streamflow depletion, $pSD_{k,t}$ at each stream segment k and time-step t , with no regard to whether
 319 there is sufficient water in the stream to meet this demand. In this section, we describe how
 320 incorporating the water available in each segment at each timestep ($WA_{k,t}$) allows us to calculate
 321 the estimated depleted streamflow ($Qd_{k,t}$) and actual streamflow depletion ($aSD_{k,t}$) for each
 322 segment and timestep as shown in Figure 1b. To do this, we consider that each stream segment
 323 has a “memory” of the amount of potential streamflow depletion that could not actually occur
 324 due to lack of instream flow, which we define as the banked depletion (BD). Initially, BD_k for
 325 each segment is zero. BD_k increases whenever $pSD_{k,t}$ exceeds $WA_{k,t}$, which occurs when instream
 326 flows are insufficient for the streamflow depletion demand. BD_k decreases when BD_k is greater
 327 than 0 and $pSD_{k,t}$ is less than $WA_{k,t}$, which occurs when there is both banked depletion and water
 328 available in the stream beyond simulated potential depletion. Specifically, the following
 329 algorithm is used to compute streamflow depletion (aSD) and streamflow (Qd) for each segment
 330 k and time t :

- 331 • Using the directed graph stream network (Figure 1b), aSD in time-step t upgradient of
 332 segment k is summed and added to the $pSD_{k,t}$ to provide the ‘cumulative potential
 333 streamflow depletion’ $CpSD_{k,t}$ in a segment:

$$334 \quad CpSD_{k,t} = pSD_{k,t} + \text{sum}[aSD_t \text{ for all segments upstream of } k] \quad \{\text{Eq. 1}\}$$

- 335 • If $CpSD_{k,t} \leq WA_{k,t}$, then:

336 ○ The actual streamflow depletion, $aSD_{k,t}$, equals the cumulative potential
 337 streamflow depletion plus any accumulated banked depletion, $BD_{k,t}$ (see below),
 338 up to the amount of water available in the stream:

$$339 \qquad aSD_{k,t} = \min[(CpSD_{k,t} + BD_{k,t}), WA_{k,t}] \qquad \{\text{Eq. 2}\}$$

340 ○ For the following time-step, $BD_{k,t+1}$ is then adjusted by the amount of delayed
 341 depletion that occurred in time-step t , unless it is zeroed out:

$$342 \qquad BD_{k,t+1} = \max[0, (BD_{k,t} - (aSD_{k,t} - CpSD_{k,t}))] \qquad \{\text{Eq. 3}\}$$

343 ● Else, if $CpSD_{k,t} > WA_{k,t}$, then:

344 ○ The actual streamflow depletion is equal to the amount of water available and the
 345 stream has dried:

$$346 \qquad aSD_{k,t} = WA_{k,t} \qquad \{\text{Eq. 4}\}$$

347 ○ The amount of potential streamflow depletion that did not occur is added to the
 348 accumulated delayed depletion available in the next time step, $BD_{k,t+1}$:

$$349 \qquad BD_{k,t+1} = BD_{k,t} + (CpSD_{k,t} - WA_{k,t}) \qquad \{\text{Eq. 5}\}$$

350 ● For each timestep, the depleted streamflow is then calculated as the difference between
 351 water available and actual streamflow depletion:

$$352 \qquad Qd_{k,t} = WA_{k,t} - aSD_{k,t} \qquad \{\text{Eq. 6}\}$$

353 ● Calculations are done sequentially, starting at the headwaters (nodes in the directed graph
 354 that do not have any inflowing segments) and moving downstream so that the actual
 355 streamflow depletion following banking and redistribution ($aSD_{k,t}$) propagates
 356 downwards to influence the timing of depletion in downstream segments.

357 3.4.3 Defining water available

358 For this study, we compared two different water available sources, which are used to
 359 represent non-depleted streamflow: SVIHM and CNFD. The simulations using SVIHM to
 360 simulate water availability are intended to maximize commensurability with SVIHM estimated
 361 streamflow depletion, allowing us to understand the differences between observed streamflow,
 362 SVIHM, and ADFs when the non-depleted streamflow is well-known. The use of CNFD data is
 363 intended to test the potential applicability to watersheds that do not have locally-developed
 364 estimates of non-depleted streamflow to help understand potential applications of ADFs for
 365 unmodeled regions.

366 From SVIHM, we used output from two specific SVIHM simulations: the calibrated
 367 basecase, with historical land use and water withdrawals for the period from 10/1/1990 to
 368 9/30/2023; and a no-groundwater-irrigation scenario, in which all model parameters and inputs
 369 are the same except that there is no groundwater pumping and groundwater-irrigation-dependent

370 crops are replaced by natural vegetation. For ADF implementation, we used the no-groundwater-
 371 irrigation scenario as our water available input. In SVIHM, we compared differences between
 372 these two scenarios to quantify the magnitude of streamflow depletion caused by groundwater
 373 pumping, incorporating differences in the water balance associated with the reversion of those
 374 fields back to natural vegetation (Barlow & Leake, 2012; Kouba & Harter, 2024; Zipper et al.,
 375 2022a). Other factors causing streamflow variability and groundwater-surface water exchange
 376 are identical to the basecase (including weather variability, surface water diversions, land use
 377 practices associated with surface water irrigation, etc). For our segment-resolution evaluation of
 378 ADF performance, we also compared ADF output with water available defined using an
 379 additional SVIHM scenario in which there was no groundwater pumping, but land use practices
 380 stayed the same throughout the watershed (i.e., groundwater-irrigated fields reverted to rainfed
 381 agriculture). While this is not a realistic agricultural practice for the region, this comparison
 382 allowed us to isolate the direct effects of pumping on streamflow, ignoring other potential
 383 changes to the water balance associated with conversion of groundwater-irrigated fields to
 384 natural vegetation. To assess the overall influence of the SVIHM scenario used for defining
 385 water available, we tested nine different SVIHM model configurations (Table S1, Figure S5,
 386 Figure S6). All SVIHM simulations used the version of the model calibrated and described by
 387 Tolley et al. (2019).

388 Table 1. Model simulations compared in this study.

Name	Streamflow depletion model	Water available source	Consideration of stream drying
ADF + SVIHM, No Drying	ADF	SVIHM, no irrigation in groundwater-dependent cropland scenario (see Table S1)	No
ADF + SVIHM + Drying	ADF	SVIHM, no irrigation in groundwater-dependent cropland scenario (see Table S1)	Yes
ADF + CNFD, No Drying	ADF	CNFD v2.1.1	No
ADF + CNFD + Drying	ADF	CNFD v2.1.1	Yes
SVIHM	SVIHM basecase with historical irrigation and land use	SVIHM, no irrigation in groundwater-dependent cropland scenario	Yes

389
 390 To assess the potential for ADF applications in locations without locally calibrated
 391 streamflow models, we used data from version 2.1.1 of the CNFD database as water available
 392 input for ADFs. This version of CNFD has a Nash-Sutcliffe Efficiency > 0.9 for the 2010-2021
 393 period via comparison to reference gages around the state. We extracted monthly CNFD
 394 predicted flow for the October 1990 to September 2023 study period at each NHD segment in the
 395 study domain. In some parts of the study domain, the NHD stream segments used in CNFD were

396 more finely discretized than the MODFLOW stream segments used by SVIHM (i.e., < 100 m
397 resolution). For these segments, we averaged the predicted unimpaired flow from CNFD
398 segments to match the spatial scale of SVIHM. This produced a timeseries of monthly CNFD
399 unimpaired flow at the same spatial resolution of SVIHM. Since CNFD does not incorporate
400 surface water diversions (which are not simulated by ADFs), we then subtracted out estimated
401 surface water diversions from SVIHM at each segment. Therefore, the ADF + CNFD
402 simulations provide an evaluation of the potential for ADFs to estimate streamflow depletion in
403 settings where non-depleted streamflow is unknown, but separate estimates of surface water
404 diversions have been developed.

405 For each water available source, we compared ADF simulations without stream drying
406 (i.e., only steps shown in Figure 1a and described in Section 3.4.1) and with stream drying (i.e.,
407 including steps shown in Figure 1b and described in Section 3.4.2). The full collection of
408 scenarios is described in Table 1.

409 *3.5 ADF model evaluation*

410 To evaluate the performance of the ADFs and the importance of incorporating stream
411 drying into these models, we evaluated a variety of variables for each model configuration in
412 Table 1. To evaluate the ability to simulate streamflow, we compared streamflow simulated by
413 ADFs and SVIHM with observations from the USGS streamflow gauging station at the
414 watershed outlet. This was primarily done at the model output timestep (5-day), though we also
415 tested fit for monthly/annual average streamflow and the number of days beneath important
416 streamflow management thresholds. Since low flows are of particular management interest in
417 this domain due to their impact on salmonid habitat, we used log-transformed streamflow,
418 referred to as $\log(\text{Streamflow})$, for our comparison. For the calculation of fit statistics when
419 streamflow was equal to 0, we added a small value (1% of the minimum observed streamflow) to
420 avoid infinite $\log(\text{Streamflow})$ values. Beyond streamflow, at the watershed outlet we compared
421 the total depletion at each timestep between ADFs and SVIHM. Throughout the network, we
422 also compared segment-resolution streamflow and streamflow depletion between the ADFs and
423 SVIHM.

424 We calculated fit statistics including the Kling-Gupta Efficiency (KGE; Gupta et al.,
425 2009), coefficient of determination (R^2), and root mean squared error as a percentage of the
426 range of observed streamflow values (normalized RMSE). The KGE is a fit statistic that
427 integrates bias, correlation, and relative variability between simulated and observed values, with
428 a KGE of 1.0 indicating a perfect agreement between simulated and observed data and $\text{KGE} < -$
429 0.41 indicating that using the mean of the observational data would be a better fit than the model
430 (Knoben et al., 2019). The R^2 represents the overall degree of correlation between the model and
431 observations. The normalized RMSE provides an indication of the degree of error in proportion
432 to the magnitude of observed variability.

433 **4. Results and Discussion**

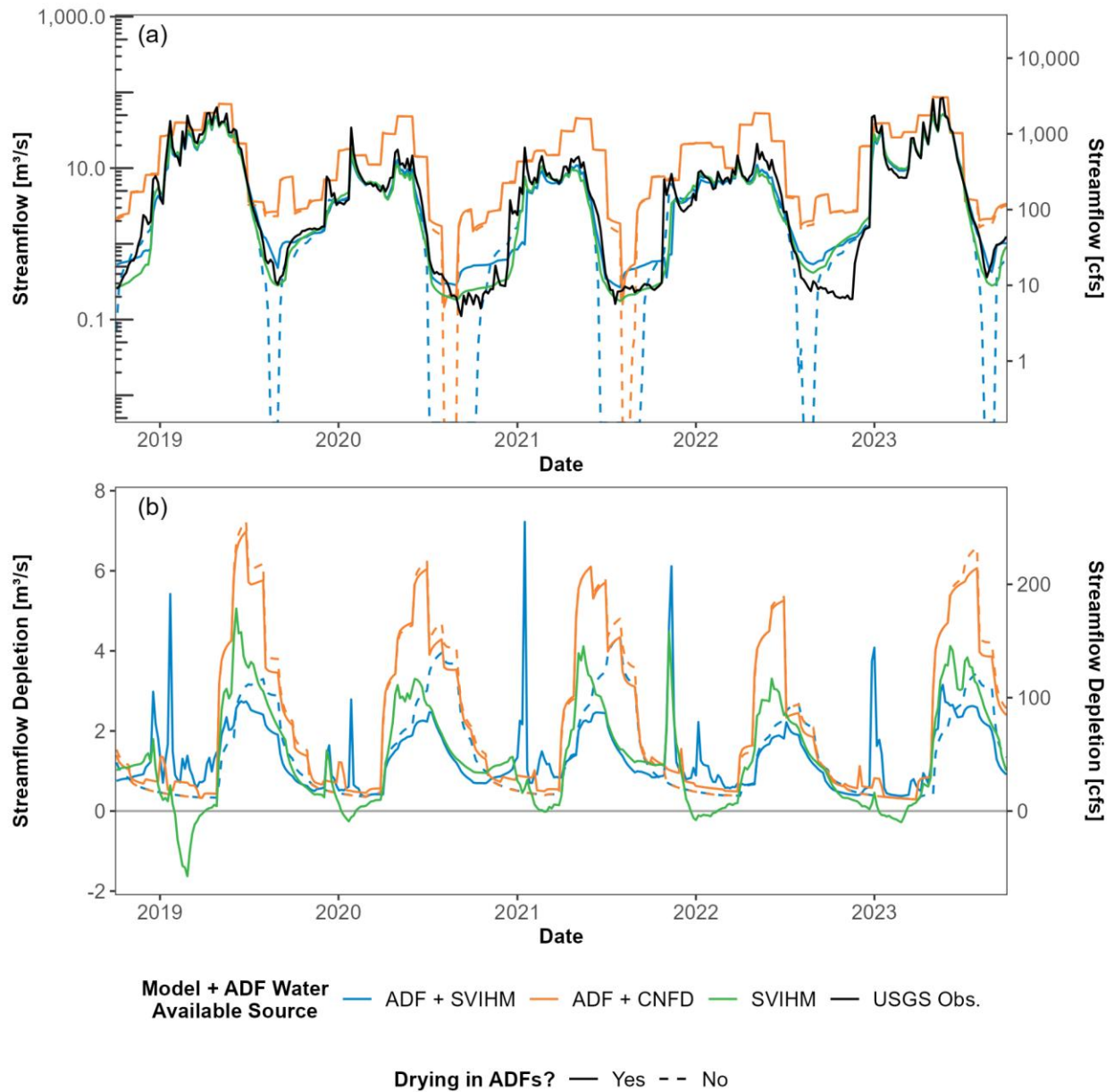
434 *4.1 Simulating streamflow and streamflow depletion at the watershed outlet*

435 The ADF + SVIHM models were able to accurately simulate both streamflow (Figure 3a,
436 Figure S1) and streamflow depletion (Figure 3b, Figure S2). Across most years, ADFs without
437 drying underestimate streamflow and overestimate streamflow depletion during summer and fall,
438 and as a result incorrectly predict that the stream should dry at the watershed outlet during the
439 summer. In contrast, the ADF + SVIHM + Drying models accurately simulate the depletion of
440 flow without drying across all years (Figure 3a). Overall, the performance of the ADF + SVIHM
441 + Drying models for simulating for $\log(\text{Streamflow})$, assessed via comparison to the USGS
442 stream gauging data, is comparable to the performance of SVIHM (Figure 4). The ADF +
443 SVIHM + Drying models have a KGE of 0.91 (compared to 0.94 for SVIHM), an R^2 of 0.92
444 (compared to 0.93 for SVIHM), and a normalized RMSE of 5.9% (compared to 6.5% for
445 SVIHM). ADF + SVIHM, No Drying models have worse fit statistics, with a KGE of 0.02, R^2 of
446 0.76, and normalized RMSE of 27.2%.

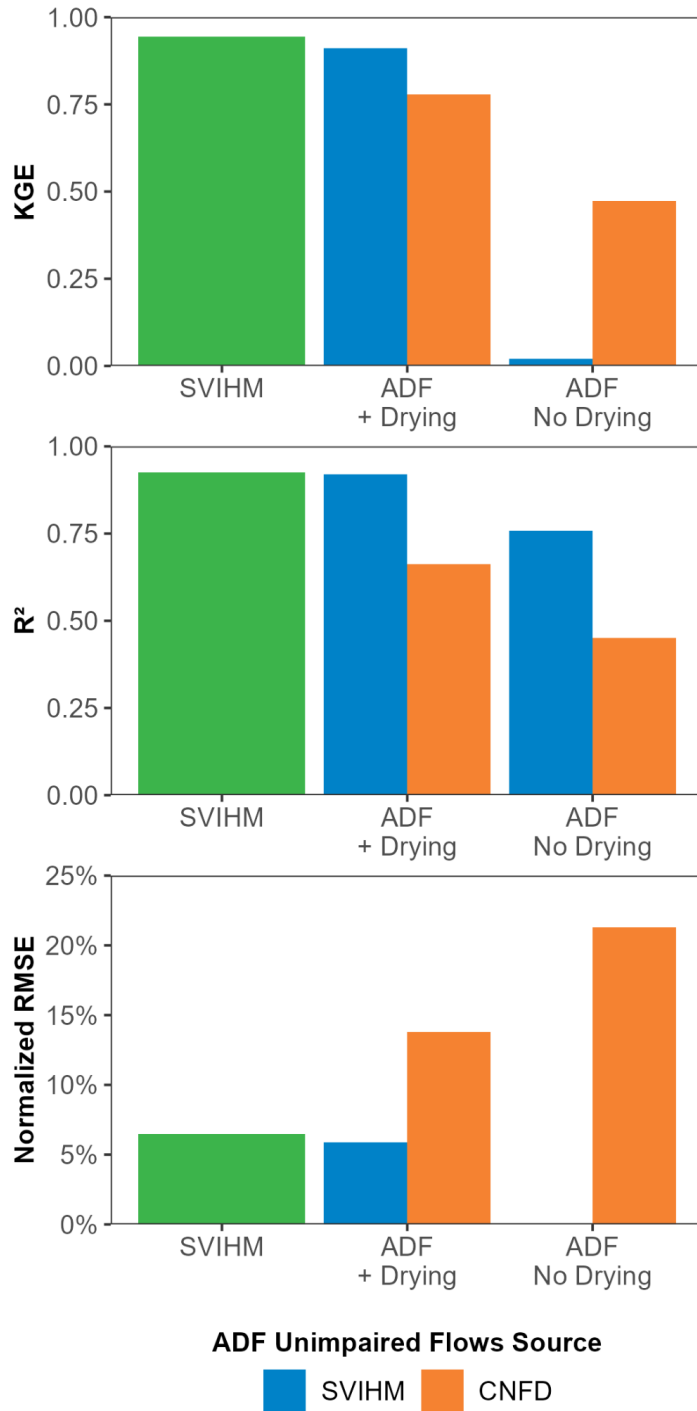
447 Due to their lower data requirements relative to numerical models, ADFs are potentially
448 useful for water management decision support in settings without existing integrated
449 groundwater-surface water models (Huggins et al., 2018; Li et al., 2022). Our ADF + CNFD
450 simulations provide one opportunity to evaluate their potential application in these settings. We
451 found that the ADF + CNFD models, which define water available based on the statewide
452 unimpaired flow model, effectively captured temporal patterns of streamflow and streamflow
453 depletion, but streamflow is biased high (Figure 3). The ADF + CNFD model results also have a
454 blockier pattern because the CNFD is a monthly model, unlike the daily SVIHM output.

455 The high bias in depleted streamflow in the ADF + CNFD model occurs because
456 unimpaired flow estimates from the CNFD model tend to be higher than the SVIHM no-
457 groundwater-irrigation scenario (Figure S5), which may result from several factors. The first is
458 that the two models are not designed to simulate the same thing. The SVIHM no-groundwater-
459 irrigation scenario still includes agricultural land cover in areas of the domain where irrigation is
460 supplied by direct surface water diversions, while the CNFD is meant to represent unimpaired
461 flow under a natural vegetation land cover and unaltered land use (though the volume of the
462 diversions is subtracted out). Non-irrigated agricultural land and an unaltered landscape without
463 modifications such as ditching would likely produce differences in the timing and magnitude of
464 fluxes such as groundwater recharge and evapotranspiration that can lead to differences in
465 streamflow, even in the absence of pumping. To assess this potential driver of differences, we
466 compared CNFD to additional SVIHM model scenarios with a variety of different natural
467 vegetation parameterizations. We found that the SVIHM natural vegetation scenarios still had a
468 lower simulated streamflow than CNFD (Figure S5). A second potential reason for disagreement
469 between these two models could be that the CNFD is trained on reference watersheds across the
470 state (Zimmerman et al., 2018), most of which are watersheds discharging from mountain
471 regions without upstream alluvial valleys. Therefore, it is possible that the important
472 hydrological processes in the Scott Valley are outside the range of training watersheds and may

473 have different dynamics that are not well-captured by CNFD. Finally, we would generally expect
 474 SVIHM to be more accurate for the Scott Valley because it is locally calibrated, while CNFD is a
 475 statewide model.



476
 477 Figure 3. Comparison of ADFs to stream gauge and numerical model data at the watershed outlet over the last 5
 478 years of the study period. (a) Streamflow. (b) Streamflow depletion. The USGS Obs. data is not included in panel
 479 (b) because streamflow depletion cannot be quantified from observational data alone. Results from all 33 study years
 480 are shown in Figure S1 and S2.
 481



482
 483
 484
 485
 486

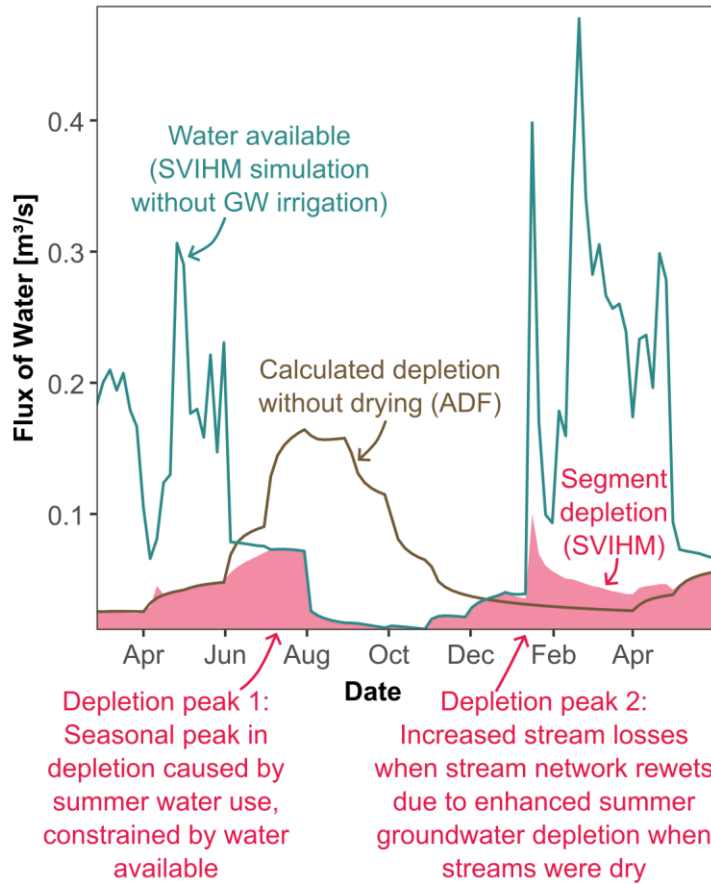
Figure 4. Model fit metrics for daily log(Streamflow), for SVIHM and ADFs with and without drying, calculated via comparison to USGS gauge at the watershed outlet. Normalized RMSE is the RMSE divided by the range of observed values. For fit statistics based on water year type, see Figure S3.

487 *4.2 Impacts of stream drying on timing and magnitude of streamflow depletion*

488 The ADF models including stream drying have better agreement with observations
489 compared to the no drying models (Figure 3, Figure 4). Simulating stream drying is critical
490 because upstream flow intermittency can lead to delays in the manifestation of streamflow
491 depletion at the watershed outlet, even if the outlet itself does not dry, due to changing stream
492 connectivity and storage dynamics within the stream network. This can lead to a behavior in
493 which there are multiple peaks in streamflow depletion within a year, including outside the
494 pumping season (Figure 3b), which has not to our knowledge been described in the literature.

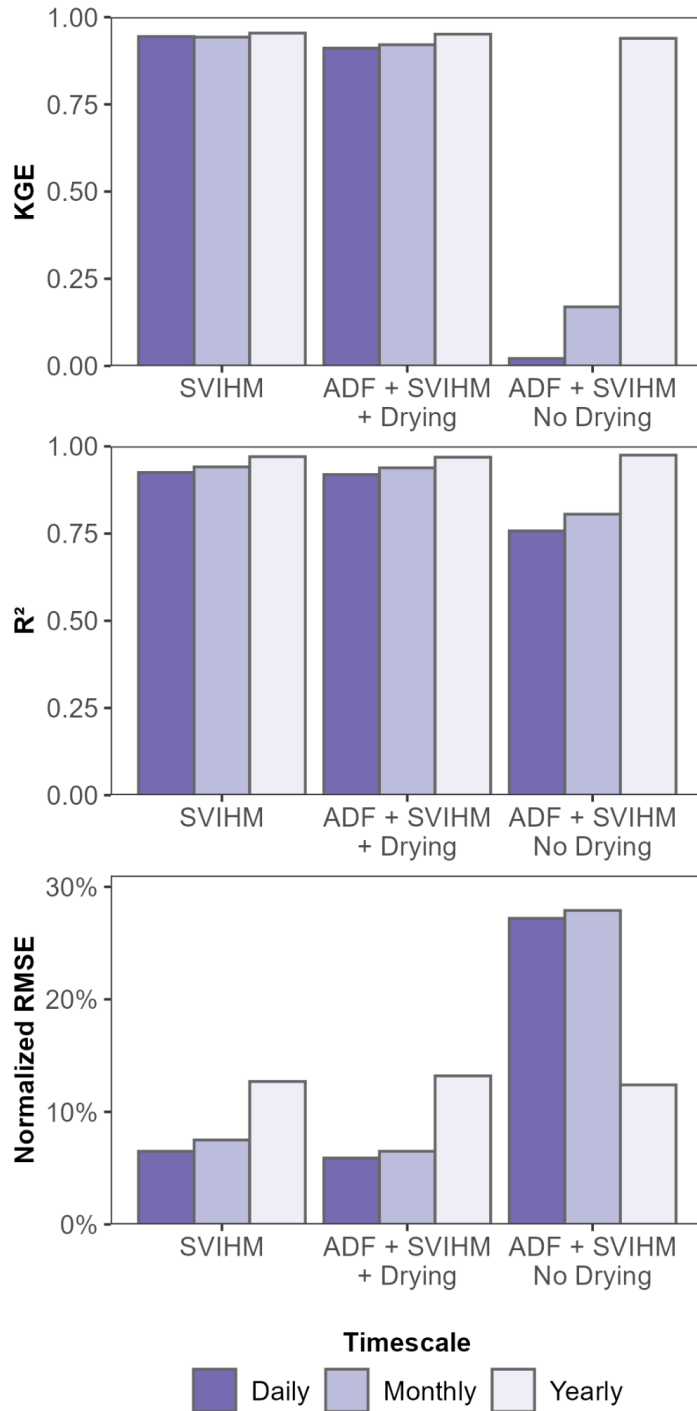
495 Mechanistically, the multiple streamflow depletion peaks are caused by changes in
496 hydrologic connectivity in both the longitudinal (upstream-downstream stream network
497 disconnection) and vertical (stream-aquifer) dimensions. In the Scott Valley, the first streamflow
498 depletion peak occurs early in the pumping season, when seasonal pumping has led to the onset
499 of streamflow depletion in the watershed but there is still sufficient surface water available from
500 snowmelt (Peak 1 in Figure 5). This pumping steadily depletes streamflow until drying occurs,
501 typically first in relatively small tributaries flowing into the main stem of the river, at which
502 points these tributaries become longitudinally disconnected from the outlet. Once the stream
503 network starts to dry, then additional pumping leads primarily to groundwater depletion, rather
504 than streamflow depletion, and the water table drops below where it would have been in a non-
505 pumped condition. As a result, once fall/winter rains begin and the stream network starts to
506 rewet, there is enhanced infiltration through the streambed in order to refill groundwater storage
507 and reconnect the stream to the aquifer (peak 2 in Figure 5). These changes in hydrologic
508 connectivity are explicitly simulated in the process-based SVIHM and reasonably reproduced in
509 the simple ADF water budget approach developed in this study (Figure 1b). Since the primary
510 impacts of drying are changes in the timing (but not total volume) of streamflow depletion,
511 incorporating these dynamics is important to simulate daily and monthly average streamflow, but
512 not critical for annual streamflow estimates (Figure 6).

513 The timing of stream drying and rewetting, and related changes in stream connectivity,
514 are critically important for local aquatic ecosystems and downstream water users (Price et al.,
515 2021, 2024). In the Scott River, the timing of the transition from the dry to wet season is a key
516 ecohydrological process supporting local salmonid populations (Kouba & Harter, 2024). Since
517 stream intermittency is globally widespread, particularly in semi-arid to arid regions where
518 irrigated agriculture is common (Hammond et al., 2021; Messenger et al., 2021; Shanafield et al.,
519 2021), it suggests these lagged depletion peaks during stream rewetting may be a common
520 phenomena that require explicit consideration when developing integrated groundwater and
521 surface water management plans (Lapides et al., 2022). The water budget-based method we
522 developed provides a parsimonious approach that appears to work well in seasonally dry
523 watersheds like the Scott River Valley. In watersheds with different drying regimes (Price et al.,
524 2021), particularly those with multi-year shifts between dry and wet regimes driven by
525 interconnections between alluvial and regional aquifer systems (Zipper et al., 2022b), additional
526 evaluation is needed to determine whether this approach is suitable.



527

528 Figure 5. Example illustrating multiple streamflow depletion peaks, which forms the basis for the ADF
 529 implementation of drying in Figure 1b. The blue line shows the SVIHM no-groundwater-irrigation scenario, which
 530 defines water available, and the red shading shows the difference between the SVIHM no-groundwater-irrigation
 531 scenario and basecase scenario, illustrating the double peak dynamics in the process-based numerical model. The
 532 brown line shows ADF estimated depletion without drying to illustrate what depletion would have been in the
 533 absence of stream drying. Data shown here are for Patterson Creek, a tributary to the Scott River on the west side of
 534 the study domain, for the March 2020 to May 2021 period. SVIHM scenarios are detailed in Table S1.
 535



536

537 Figure 6. Model fit metrics based on timescale of comparison for log(Streamflow), for SVIHM and ADFs with and
 538 and without drying, calculated via comparison to USGS gauge at the watershed outlet. ADFs shown here are using the
 539 SVIHM no-groundwater-irrigation scenario as available water. Normalized RMSE is the RMSE divided by the
 540 range of observed values. The Yearly fit is calculated as April-March average streamflow, based on the timing of the
 541 onset of seasonal pumping in the watershed.
 542

543 *4.2 Simulating streamflow and streamflow depletion throughout the watershed*

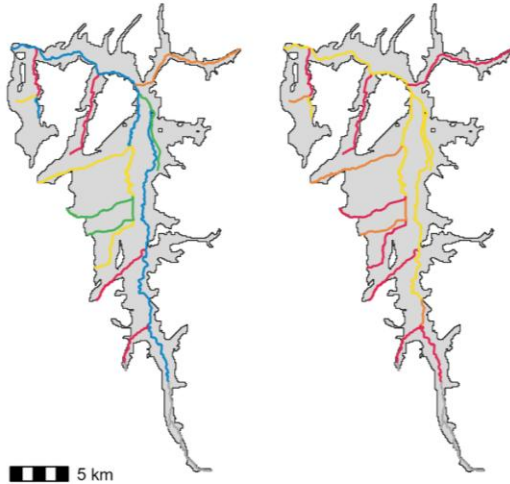
544 To evaluate the accuracy and utility of ADFs throughout the Scott Valley watershed,
545 including in settings where there was no stream gauging data available, we compared segment-
546 resolution ADF + SVIHM + Drying output to results from SVIHM. We excluded stream
547 segments where SVIHM results indicated depletion was $< 1\%$ of non-depleted streamflow $>$
548 90% of the time to focus only on locations with pumping impacts. We found that agreement
549 between the two modeling approaches was generally good ($KGE > 0$) to excellent ($KGE > 0.5$)
550 for $\log(\text{Streamflow})$ when using the SVIHM no-groundwater-irrigation scenario to define ADF
551 water available (Figure 7a). Agreement in terms of streamflow depletion (Figure 7b) was worse
552 than agreement for streamflow, primarily in tributary regions, but generally had $KGE > 0.5$ along
553 the main stem of the Scott River.

554 We also compared streamflow depletion using an alternate SVIHM parameterization, in
555 which pumping was turned off but groundwater-irrigated areas remained in agricultural land
556 cover (scenario #2 from Table S1). This allows us to isolate the impacts of groundwater pumping
557 on streamflow in SVIHM, which provides a more commensurate comparison to ADF results
558 which directly simulate the impacts of pumping (not land use change) on streamflow. We found
559 that agreement in simulated streamflow depletion was much stronger (Figure 7d), with only a
560 slight degradation in simulated streamflow (Figure 7c). This comparison among SVIHM
561 scenarios suggests that the application of ADFs for management decision-making should be
562 aligned with their structure and assumptions. Since ADFs directly simulate streamflow depletion
563 caused by changes in pumping and do not simulate other changes in the water balance associated
564 with conversion between natural and agricultural land cover, they are better-suited to assess the
565 impacts of changes in pumping under constant land cover scenarios rather than holistic changes
566 in the water balance associated with native vegetation restoration in irrigated landscapes.
567 However, if independent estimates of changes in consumptive water use could be developed (for
568 example, through approaches like remote sensing of evapotranspiration), these water balance
569 changes could be integrated with ADF-based estimates of pumping impacts on streamflow to
570 provide a full accounting of changes in the water balance and impacts on streamflow.

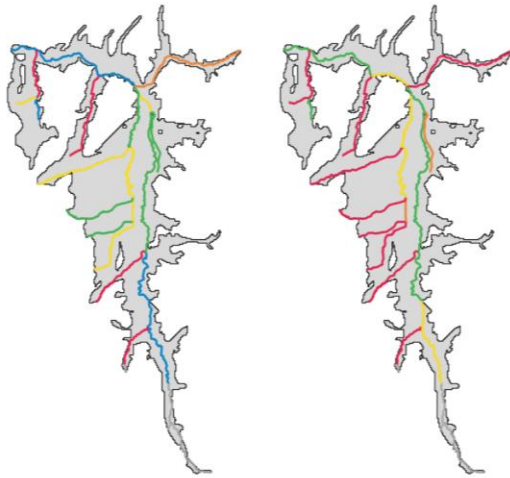
571 Agreement for both streamflow and streamflow depletion tends to be best for the higher-
572 flow and more heavily-depleted segments along the main stem (Figure 7, Figure S7) and worst in
573 isolated tributaries where there is little flow and little depletion. In tributaries, ADFs estimates of
574 streamflow depletion tended to be greater than SVIHM and therefore streamflow estimates were
575 lower than SVIHM including simulating more frequent drying than SVIHM. However, the
576 strong agreement in the more heavily-depleted areas means that ADFs are capturing the large
577 majority of pumping impacts accurately. KGE is > 0.5 in $\sim 55\%$ of the segments for
578 $\log(\text{Streamflow})$ (Figure 8a), and these segments represent $> 80\%$ of total streamflow depletion in
579 the domain (Figure 8b). Similarly, KGE is > 0.5 in $\sim 25\%$ of segments for streamflow depletion
580 (Figure 8a), but these represent $\sim 70\%$ of the total streamflow depletion in the domain (Figure
581 8b). This indicates that the impacts of pumping are best-simulated by ADFs in the settings where
582 depletion is greatest and accuracy is most important. In sum, the ADF simulations are able to

583 effectively simulate both the magnitude and spatial distribution of streamflow depletion in this
584 domain.

(a) log(Streamflow) (b) Streamflow Depletion
Water Available = SVIHM No GW Irrigation scenario

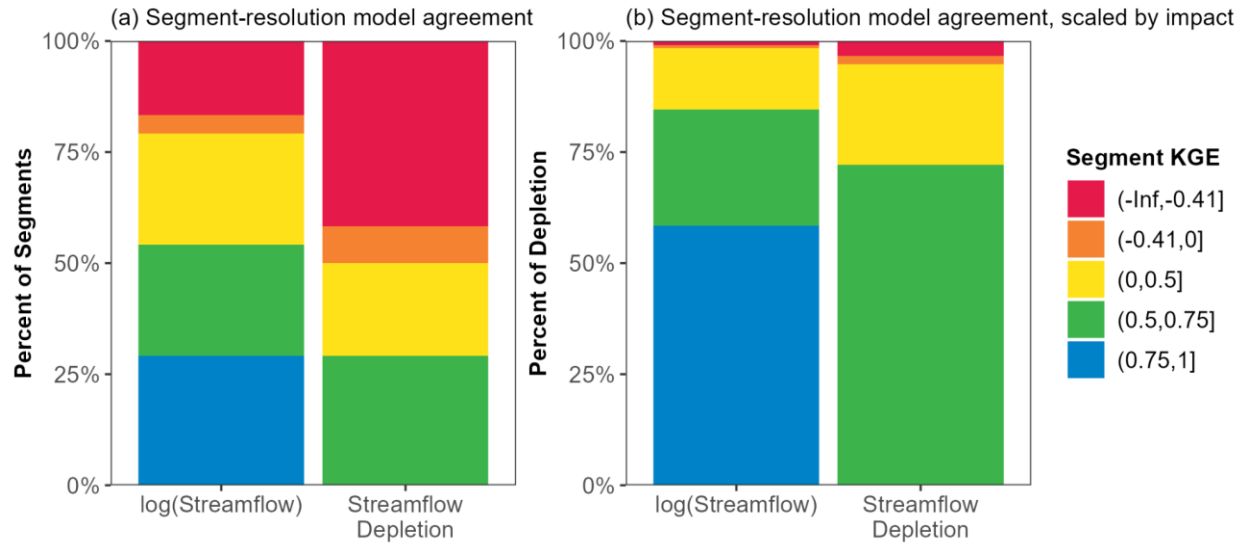


(c) log(Streamflow) (d) Streamflow Depletion
Water Available = SVIHM No Pumping scenario



KGE — (-Inf,-0.41] — (-0.41,0] — (0,0.5] — (0.5,0.75] — (0.75,1]

585
586 Figure 7. Distribution of segment-resolution agreement between ADFs and SVIHM for (a) streamflow and (b)
587 streamflow depletion. ADF models shown here include drying. Panels (a) and (b) use the SVIHM no groundwater
588 irrigation scenario (#3b from Table S1) and panels (c) and (d) use the SVIHM no pumping scenario (#2 from Table
589 S1). A KGE < -0.41 indicates that the model performs worse than using the mean of observational data (Knoben et
590 al., 2019).
591



592
 593 Figure 8. Segment-resolution agreement between ADFs and SVIHM, expressed as (a) the percentage of the number
 594 of segments in the model domain and (b) the percentage of mean simulated streamflow depletion (from SVIHM)
 595 in the model domain. NA values indicate segments where a KGE could not be calculated because the ADFs did not
 596 simulate any depletion, which are the two segments at the southern inlet to Scott Valley. These results show the
 597 ADF + SVIHM + Drying model configuration with water available and SVIHM streamflow depletion calculated
 598 using the the SVIHM no-pumping scenario (#2 in Table S1), as visualized in Figure 7c-d.

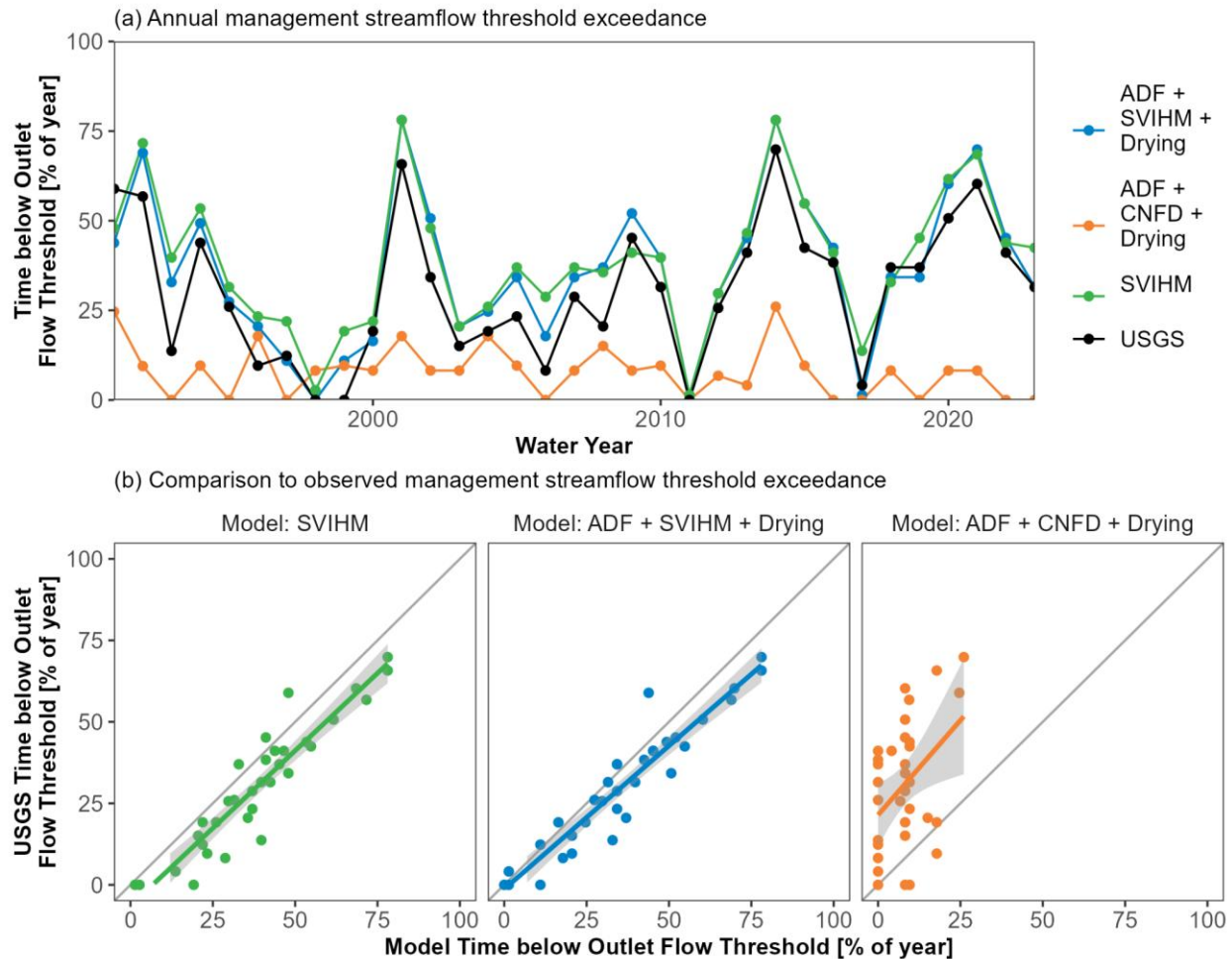
599
 600 *4.3 Integration with water management decision-making*

601 4.3.1 Simulation of critical streamflow management thresholds

602 Accurate estimates of streamflow depletion are critical to effective integrated
 603 groundwater and surface water management. To determine if ADFs have sufficient accuracy to
 604 support local ecohydrological management decisions, we evaluated their ability to simulate the
 605 duration of streamflow below monthly minimum streamflow requirements for the gauging
 606 station at the Scott Valley watershed outlet. These streamflow thresholds are designed to provide
 607 ecological flows sufficient for salmonid survival at all life stages and vary throughout the year
 608 (Figure S8), from a minimum of 0.85 m³/sec (30 ft³/sec) in August to a maximum of 5.7 m³/sec
 609 (200 ft³/sec) in January (California State Water Resources Control Board [SWRCB], 2025). The
 610 monthly minimum streamflow requirements were developed in 2021 by the SWRCB, as
 611 recommended by the California Department of Fish and Wildlife in coordination with the
 612 National Marine Fisheries Service, and were readopted in 2022, 2024, and 2025 under additional
 613 drought emergency regulations. Under emergency drought regulations, the SWRCB has the right
 614 to curtail water users if Scott River flows fall below minimum flow requirements. As of 2025,
 615 the SWRCB is in the process of pursuing the development and implementation of permanent
 616 instream minimum flow requirements for the Scott River. As a result, the ability of streamflow
 617 depletion models to accurately estimate streamflow relative to these minimum instream flow
 618 thresholds is critical to water resources management and the future development of decision-
 619 support tools.

620 The ADF + SVIHM + Drying models are able to simulate the annual duration of
621 threshold exceedance with comparable accuracy to the locally-calibrated SVIHM model (Figure
622 9). Overall the duration of model-simulated threshold exceedance agrees well with observations,
623 with a mean absolute error (MAE) of 7.3% for the ADF + SVIHM + Drying model and 9.5% for
624 the SVIHM model. In general, the models (both SVIHM and ADF + SVIHM + Drying) tend to
625 simulate slightly more threshold exceedance than was observed during dry years, but the greatest
626 discrepancy was in the relatively wet year of 2019. In 2019, both SVIHM and ADF + SVIHM +
627 Drying models substantially underestimated the frequency of threshold exceedance (observed =
628 37.0% of days below threshold, SVIHM = 5.5%, ADF + SVIHM + Drying = 2.7% of days).

629 For basins without locally calibrated models, which are areas that ADFs can provide low-
630 cost estimates of streamflow and streamflow depletion, local estimates of water available without
631 pumping are necessary to convert depletion calculated by ADFs to streamflow and, if needed,
632 redistribute in time to account for stream drying. We tested the applicability of the CNFD for this
633 purpose, and found that threshold exceedance predicted by the ADF + CNFD + Drying models
634 was positively correlated ($r = 0.42$) with the observed threshold exceedance, but the percent of
635 time exceeding the thresholds is lower in the ADF + CNFD + Drying model (MAE = 24%;
636 Figure 10b). This is due to the fact that the CNFD unimpaired flow estimates are higher than the
637 SVIHM no-groundwater-irrigation scenario (Figure S5), as discussed in Section 4.1. As a result,
638 depleted streamflow in the ADF + CNFD + Drying models tends to remain above the in-stream
639 flow thresholds for the majority of the year, even during dry conditions like 2015 and 2021.



640
 641 Figure 10. (a) Number of days per year with watershed outlet streamflow below California Department of Fish and
 642 Wildlife management thresholds for each modeling approach and USGS observed flow. (b) Comparison of each
 643 modeling approach to USGS observations. ADF simulations plotted here include drying.
 644

645 4.3.2 Extension to unmodeled watersheds

646 To extend the capabilities of ADFs to watersheds that do not have locally-calibrated
 647 streamflow models, there are multiple potential approaches that could be explored to develop
 648 reliable water available estimates. In California, regional statistical models like CNFD are
 649 available, and in other domains there is an increasing abundance of data-driven models that have
 650 primarily been trained on reference watersheds at national to global scales and therefore could
 651 provide local non-pumped streamflow estimates (Kratzert et al., 2019, 2022). Data-driven
 652 modeling, to date, has primarily focused on reference watersheds and therefore predictions from
 653 these models for ungauged basins may be representative of non-depleted streamflow. There are
 654 also an increasing number of regional- to national-scale process-based models, such as the
 655 National Hydrologic Model (NHM; Regan et al., 2019) or ParFlow-CONUS (Condon &
 656 Maxwell, 2019; Maxwell et al., 2015). Since many national-scale models do not explicitly
 657 incorporate groundwater pumping (Bosompemaa et al., 2025; Towler et al., 2023), or can be run

658 in both pumping-on and pumping-off configurations (Condon & Maxwell, 2019), their flow
659 estimates could provide a useful water available input for the ADF models.

660 Regardless of the water available source, incorporating a local calibration and bias
661 correction approach into ADF workflows would likely improve local relevance and better match
662 observed streamflow. The ADFs used in this study are not calibrated, though they use calibrated
663 model parameters from SVIHM as inputs. In most settings, hydrostratigraphic inputs (such as
664 transmissivity and storativity) and ADF-specific parameters (such as the weighting factor for
665 depletion apportionment) will need to be estimated and refined based on local data. As part of
666 this process, ADF models could be calibrated to improve agreement with observed streamflow
667 data, as is typically done for numerical models of streamflow depletion (Barlow et al., 2018;
668 Fienen et al., 2018; Foster et al., 2021). For ungauged areas where no gauging station is available
669 for calibration, additional work would be needed to identify locally-appropriate refinements, for
670 example through parameter regionalization (Bawa et al., 2025; Beck et al., 2016; Mihret et al.,
671 2025).

672 4.3.3 Integrating multiple modeling approaches to meet management needs

673 Streamflow depletion cannot be measured directly at the scales relevant to regional water
674 resource management, and therefore modeling tools must be developed to support decision-
675 making (Zipper et al., 2024). While a globally relevant issue, this technical need has recently
676 emerged within two management contexts in California. As previously mentioned, assessing
677 depletion of interconnected surface waters is a requirement under SGMA, and many
678 groundwater managers across the state must develop models capable of estimating streamflow
679 depletion. Additionally, courts in California have recently ruled that groundwater withdrawals
680 are subject to regulation under the Public Trust Doctrine on the basis that groundwater
681 withdrawals have the potential to harm navigable waterways (*Environmental Law Foundation v.*
682 *State Water Resources Control Board*, 2018). This has resulted in county agency efforts to revise
683 well permitting regulations, and has highlighted the need for modeling tools to estimate potential
684 impacts of streamflow depletion on public trust resources such as navigable waters or aquatic
685 ecosystems.

686 In many management contexts, it is likely that a combination of analytical and numerical
687 methods will be implemented statewide as groundwater managers balance resource constraints
688 (time, cost, available technical expertise, risk of significant impacts, etc., as discussed in Zipper
689 et al., 2022a). Our analysis demonstrates that ADFs may be implemented effectively as low-
690 complexity, low-cost techniques in hydrogeologic settings where their simplifying assumptions
691 hold (i.e. alluvial groundwater subbasins where a high degree of interconnectivity between
692 surface and groundwater resources exist) and can be accurately extended outside these conditions
693 where reasonable process-representations can be developed, as we demonstrate with our
694 simplified approach for stream drying (Figure 1b). This emerging modeling framework is
695 promising based upon its ability to be developed as a cost-effective solution to estimating
696 streamflow depletion due to groundwater pumping and potential integration into web-based
697 decision support tools (Huggins et al., 2018). Numerical models will continue to be key tools in

698 complex settings where water resources management decision-making benefits from a detailed
699 representation of water balance dynamics or necessitates complex management scenario
700 simulations (managed aquifer recharge, phreatophytic evapotranspiration dynamics, reservoir
701 operations). A unified modeling philosophy that utilizes a suite of streamflow depletion
702 modeling methods in varying contexts will provide groundwater managers with the flexibility to
703 develop decision-support tools appropriate to the scope of their specific needs.

704

705 **5. Conclusions**

706 Analytical depletion functions (ADFs) are a low-complexity and scalable approach that
707 provide accurate estimates of both streamflow and streamflow depletion for the Scott River
708 Valley. We find that ADF estimates of streamflow are comparable to observed streamflow from
709 a USGS gauging station at the watershed outlet and to simulated streamflow by SVIHM, a
710 process-based integrated hydrologic model developed for the watershed. ADFs also accurately
711 predict how frequently streamflow drops below critical management thresholds. However,
712 developing accurate estimates of streamflow and streamflow depletion using ADFs requires a
713 locally accurate estimate of non-depleted streamflow (what streamflow would have been without
714 groundwater pumping). ADFs simulate the direct effects of pumping on streamflow, and do not
715 explicitly account for other changes in the water balance caused by the conversion of natural
716 vegetation to irrigated agriculture, and therefore may be best-suited to quantify the marginal
717 impacts of changes in pumping on streamflow unless independent estimates of additional water
718 balance changes can be estimated, for example using remotely sensed estimates of differences in
719 consumptive water use. We show that using a regional statistical model, the California Natural
720 Flows Database (CNFD), provided reasonable temporal dynamics, but estimated non-depleted
721 streamflow by CNFD is higher than the non-depleted streamflow simulated by SVIHM. As a
722 result, ADFs using CNFD as an input overestimate streamflow. This suggests that developing an
723 approach to locally calibrate and refine ADFs using CNFD may have potential for for
724 streamflow depletion assessments in ungauged and unmodeled watersheds within California, and
725 has potential for application elsewhere using data-driven or process-based streamflow models to
726 represent water available.

727 Incorporating stream drying, and associated temporal redistribution of streamflow
728 depletion, is critical to accurately estimate streamflow and streamflow depletion in this domain at
729 sub-annual scales. We demonstrate that reductions in hydrologic connectivity caused by stream
730 drying can lead to substantial lags in the manifestation of streamflow depletion. These lags occur
731 because, when the streams dry, continued pumping leads to increased groundwater depletion as
732 the stream and aquifer are disconnected. When the hydrologic system rewets in the fall/winter
733 rainy season, there are greater stream losses due to increased infiltration through the streambed
734 until the depleted groundwater system is replenished and the stream-aquifer system is
735 reconnected. We incorporate this process into ADF models using a simple water budget
736 approach at the stream reach resolution, and route the resulting changes in the timing of
737 streamflow downstream through the river network and show strong agreement with both SVIHM

738 and observed streamflow. These findings advance ADFs towards potential application as a water
739 management decision-support tool.

740 **Acknowledgments**

741 We appreciate useful feedback from Ben Kerr, Laura Foglia, Matt O'Connor, Jeremy Kobor, and
742 others.

743 **Data and Code Availability**

744 ADFs are available in the streamDepletr package for R: [https://cran.r-](https://cran.r-project.org/package=streamDepletr)
745 [project.org/package=streamDepletr](https://cran.r-project.org/package=streamDepletr)

746 SVIHM is available at: <https://github.com/scantle/SVIHM>

747 The data and code used in this study are available on HydroShare:

748 <http://www.hydroshare.org/resource/f36f9b62549c46498bba89db66a8cbc5>

749 **Funding**

750 This work was supported by The Nature Conservancy grants #10192023-16680 and #06132024-
751 17291 to SZ.

752 **Declaration of interests**

753 The authors have nothing to declare.

754 **Declaration of generative AI and AI-assisted technologies in the writing process**

755 During the preparation of this work the author(s) used ChatGPT in order to explore alternate
756 programming approaches to create directed stream network graphs and incorporate stream
757 drying, which were then tested by the author(s) for suitability and efficiency. After using this
758 tool/service, the author(s) reviewed and edited the content as needed and take(s) full
759 responsibility for the content of the published article.

760 **Author contributions**

761 SZ: Conceptualization, Data curation, Formal Analysis, Funding acquisition, Investigation,
762 Methodology, Project administration, Software, Supervision, Validation, Visualization, Writing
763 – original draft, Writing – review & editing

764
765 IG: Data curation, Formal Analysis, Investigation, Methodology, Software, Visualization,
766 Writing – review & editing

767
768 NM: Conceptualization, Data curation, Funding acquisition, Investigation, Methodology, Project
769 administration, Writing – original draft, Writing – review & editing

770
771 MS: Conceptualization, Funding acquisition, Methodology, Project administration, Writing –
772 review & editing

773

774 CK: Data curation, Methodology, Investigation, Software, Validation, Writing – review &
775 editing
776
777 LS: Data curation, Methodology, Investigation, Software, Validation, Writing – original draft,
778 Writing – review & editing
779
780 TH: Funding acquisition, Methodology, Supervision, Writing – review & editing
781

782 References

- 783 Abimbola, O. P., Mittelstet, A. R., & Gilmore, T. E. (2020a). Geostatistical features of streambed
784 vertical hydraulic conductivities in Frenchman Creek Watershed in Western Nebraska.
785 *Hydrological Processes*, 34(16), 3481–3491. <https://doi.org/10.1002/hyp.13823>
- 786 Abimbola, O. P., Mittelstet, A. R., Gilmore, T. E., & Korus, J. T. (2020b). Influence of
787 watershed characteristics on streambed hydraulic conductivity across multiple stream
788 orders. *Scientific Reports*, 10(1), 3696. <https://doi.org/10.1038/s41598-020-60658-3>
- 789 Barlow, P. M., Leake, S. A., & Fienen, M. N. (2018). Capture Versus Capture Zones: Clarifying
790 Terminology Related to Sources of Water to Wells. *Groundwater*, 56(5), 694–704.
791 <https://doi.org/10.1111/gwat.12661>
- 792 Barlow, P. M., & Leake, S. A. (2012). *Streamflow depletion by wells--Understanding and*
793 *managing the effects of groundwater pumping on streamflow* (No. Circular 1376). Reston
794 VA: U.S. Geological Survey. Retrieved from <https://pubs.usgs.gov/circ/1376/>
- 795 Bawa, A., Mendoza, K., Srinivasan, R., O'Donchha, F., Smith, D., Wolfe, K., Parmar, R.,
796 Johnston, J. M., & Corona, J. (2025). Enhancing hydrological modeling of ungauged
797 watersheds through machine learning and physical similarity-based regionalization of
798 calibration parameters. *Environmental Modelling & Software*, 186, 106335.
799 <https://doi.org/10.1016/j.envsoft.2025.106335>
- 800 Beck, H. E., van Dijk, A. I. J. M., de Roo, A., Miralles, D. G., McVicar, T. R., Schellekens, J., &
801 Bruijnzeel, L. A. (2016). Global-scale regionalization of hydrologic model parameters.
802 *Water Resources Research*, 52(5), 3599–3622. <https://doi.org/10.1002/2015WR018247>
- 803 Bosompemaa, P., Brookfield, A., Zipper, S., & Hill, M. C. (2025). Using national hydrologic
804 models to obtain regional climate change impacts on streamflow basins with
805 unrepresented processes. *Environmental Modelling & Software*, 183, 106234.
806 <https://doi.org/10.1016/j.envsoft.2024.106234>
- 807 California Department of Water Resources. (2024). *Depletion of Interconnected Surface Water:*
808 *An Introduction*. Retrieved from [https://data.cnra.ca.gov/dataset/68e0d8b6-a207-4b30-](https://data.cnra.ca.gov/dataset/68e0d8b6-a207-4b30-a16b-3daeb659faea/resource/218e3361-c142-400f-a97f-5dfa79cd4997/download/depletionsofisw_paper1_intro_draft.pdf)
809 [a16b-3daeb659faea/resource/218e3361-c142-400f-a97f-](https://data.cnra.ca.gov/dataset/68e0d8b6-a207-4b30-a16b-3daeb659faea/resource/218e3361-c142-400f-a97f-5dfa79cd4997/download/depletionsofisw_paper1_intro_draft.pdf)
810 [5dfa79cd4997/download/depletionsofisw_paper1_intro_draft.pdf](https://data.cnra.ca.gov/dataset/68e0d8b6-a207-4b30-a16b-3daeb659faea/resource/218e3361-c142-400f-a97f-5dfa79cd4997/download/depletionsofisw_paper1_intro_draft.pdf)
- 811 California State Water Resources Control Board. (2025). *Finding of Emergency and Informative*
812 *Digest: Proposed Scott River and Shasta River Watersheds Emergency Regulation*.
813 Sacramento CA: California State Water Resources Control Board. Retrieved from
814 [https://www.waterboards.ca.gov/drought/scott_shasta_rivers/docs/2025/scott-shasta-](https://www.waterboards.ca.gov/drought/scott_shasta_rivers/docs/2025/scott-shasta-drought-informative-digest.pdf)
815 [drought-informative-digest.pdf](https://www.waterboards.ca.gov/drought/scott_shasta_rivers/docs/2025/scott-shasta-drought-informative-digest.pdf)
- 816 Christensen, S. (2000). On the Estimation of Stream Flow Depletion Parameters by Drawdown
817 Analysis. *Groundwater*, 38(5), 726–734. [https://doi.org/10.1111/j.1745-](https://doi.org/10.1111/j.1745-6584.2000.tb02708.x)
818 [6584.2000.tb02708.x](https://doi.org/10.1111/j.1745-6584.2000.tb02708.x)
- 819 Condon, L. E., & Maxwell, R. M. (2019). Simulating the sensitivity of evapotranspiration and

820 streamflow to large-scale groundwater depletion. *Science Advances*, 5(6), eaav4574.
821 <https://doi.org/10.1126/sciadv.aav4574>

822 Datry, T., Truchy, A., Olden, J. D., Busch, M. H., Stubbington, R., Dodds, W. K., Zipper, S., Yu,
823 S., Messenger, M. L., Tonkin, J. D., Kaiser, K. E., Hammond, J. C., Moody, E. K.,
824 Burrows, R. M., Sarremejane, R., DelVecchia, A. G., Fork, M. L., Little, C. J., ... Allen,
825 D. (2022). Causes, Responses, and Implications of Anthropogenic versus Natural Flow
826 Intermittence in River Networks. *BioScience*, biac098.
827 <https://doi.org/10.1093/biosci/biac098>

828 Environmental Law Foundation v. State Water Resources Control Board, 26 Cal.App.5th 844
829 Cal. Rptr. 3d 393 237 (Cal. Ct. App. 2018).

830 Falke, J. A., Fausch, K. D., Magelky, R., Aldred, A., Durnford, D. S., Riley, L. K., & Oad, R.
831 (2011). The role of groundwater pumping and drought in shaping ecological futures for
832 stream fishes in a dryland river basin of the western Great Plains, USA. *Ecohydrology*,
833 4(5), 682–697. <https://doi.org/10.1002/eco.158>

834 Fienen, M. N., Bradbury, K. R., Kniffin, M., & Barlow, P. M. (2018). Depletion Mapping and
835 Constrained Optimization to Support Managing Groundwater Extraction. *Groundwater*,
836 56(1), 18–31. <https://doi.org/10.1111/gwat.12536>

837 Flores, L., Bailey, R. T., & Kraeger-Rovey, C. (2020). Analyzing the Effects of Groundwater
838 Pumping on an Urban Stream-Aquifer System. *JAWRA Journal of the American Water
839 Resources Association*, 56(2), 310–322. <https://doi.org/10.1111/1752-1688.12827>

840 Foglia, L., McNally, A., & Harter, T. (2013). Coupling a spatiotemporally distributed soil water
841 budget with stream-depletion functions to inform stakeholder-driven management of
842 groundwater-dependent ecosystems. *Water Resources Research*, 49(11), 7292–7310.
843 <https://doi.org/10.1002/wrcr.20555>

844 Foglia, L., Neumann, J., Tolley, D., Orloff, S., Snyder, R., & Harter, T. (2018). Modeling guides
845 groundwater management in a basin with river–aquifer interactions. *California
846 Agriculture*, 72(1), 84–95.

847 Foster, L. K., White, J. T., Leaf, A. T., Houston, N. A., & Teague, A. (2021). Risk-Based
848 Decision-Support Groundwater Modeling for the Lower San Antonio River Basin, Texas,
849 USA. *Groundwater*, 59(4), 581–596. <https://doi.org/10.1111/gwat.13107>

850 Gage, A., & Milman, A. (2020). Groundwater Plans in the United States: Regulatory
851 Frameworks and Management Goals. *Groundwater*. <https://doi.org/10.1111/gwat.13050>

852 Glover, R. E., & Balmer, G. G. (1954). River depletion resulting from pumping a well near a
853 river. *Eos, Transactions American Geophysical Union*, 35(3), 468–470.
854 <https://doi.org/10.1029/TR035i003p00468>

855 Grantham, T. E., Carlisle, D. M., Howard, J., Lane, B., Lusardi, R., Obester, A., Sandoval-Solis,
856 S., Stanford, B., Stein, E. D., Taniguchi-Quan, K. T., Yarnell, S. M., & Zimmerman, J. K.
857 H. (2022). Modeling Functional Flows in California’s Rivers. *Frontiers in Environmental
858 Science*, 10. <https://doi.org/10.3389/fenvs.2022.787473>

859 Gupta, H. V., Kling, H., Yilmaz, K. K., & Martinez, G. F. (2009). Decomposition of the mean
860 squared error and NSE performance criteria: Implications for improving hydrological
861 modelling. *Journal of Hydrology*, 377(1), 80–91.
862 <https://doi.org/10.1016/j.jhydrol.2009.08.003>

863 Hammond, J. C., Zimmer, M., Shanafield, M., Kaiser, K., Godsey, S. E., Mims, M. C., Zipper, S.
864 C., Burrows, R. M., Kampf, S. K., Dodds, W., Jones, C. N., Krabbenhoft, C. A.,
865 Boersma, K. S., Datry, T., Olden, J. D., Allen, G. H., Price, A. N., Costigan, K., ... Allen,

- 866 D. C. (2021). Spatial Patterns and Drivers of Nonperennial Flow Regimes in the
867 Contiguous United States. *Geophysical Research Letters*, 48(2), e2020GL090794.
868 <https://doi.org/10.1029/2020GL090794>
- 869 Hantush, M. S. (1965). Wells near streams with semipervious beds. *Journal of Geophysical*
870 *Research*, 70(12), 2829–2838. <https://doi.org/10.1029/JZ070i012p02829>
- 871 Harter, T. (2020). California’s 2014 Sustainable Groundwater Management Act – From the Back
872 Seat to the Driver Seat in the (Inter)National Groundwater Sustainability Movement. In
873 J.-D. Rinaudo, C. Holley, S. Barnett, & M. Montginoul (Eds.), *Sustainable Groundwater*
874 *Management: A Comparative Analysis of French and Australian Policies and*
875 *Implications to Other Countries* (pp. 511–536). Cham: Springer International Publishing.
876 https://doi.org/10.1007/978-3-030-32766-8_26
- 877 Huang, C.-S., Yang, T., & Yeh, H.-D. (2018). Review of analytical models to stream depletion
878 induced by pumping: Guide to model selection. *Journal of Hydrology*, 561, 277–285.
879 <https://doi.org/10.1016/j.jhydrol.2018.04.015>
- 880 Huggins, X., Gleeson, T., Eckstrand, H., & Kerr, B. (2018). Streamflow Depletion Modeling:
881 Methods for an Adaptable and Conjunctive Water Management Decision Support Tool.
882 *JAWRA Journal of the American Water Resources Association*, 54(5), 1024–1038.
883 <https://doi.org/10.1111/1752-1688.12659>
- 884 Hunt, B. (1999). Unsteady Stream Depletion from Ground Water Pumping. *Ground Water*,
885 37(1), 98–102. <https://doi.org/10.1111/j.1745-6584.1999.tb00962.x>
- 886 Hunt, B., Weir, J., & Clausen, B. (2001). A Stream Depletion Field Experiment. *Ground Water*,
887 39(2), 283–289. <https://doi.org/10.1111/j.1745-6584.2001.tb02310.x>
- 888 Kallis, G., & Butler, D. (2001). The EU water framework directive: measures and implications.
889 *Water Policy*, 3(2), 125–142. [https://doi.org/10.1016/S1366-7017\(01\)00007-1](https://doi.org/10.1016/S1366-7017(01)00007-1)
- 890 Knoben, W. J. M., Freer, J. E., & Woods, R. A. (2019). Technical note: Inherent benchmark or
891 not? Comparing Nash–Sutcliffe and Kling–Gupta efficiency scores. *Hydrology and Earth*
892 *System Sciences*, 23(10), 4323–4331. <https://doi.org/10.5194/hess-23-4323-2019>
- 893 Kollet, S. J., & Zlotnik, V. A. (2003). Stream depletion predictions using pumping test data from
894 a heterogeneous stream–aquifer system (a case study from the Great Plains, USA).
895 *Journal of Hydrology*, 281(1), 96–114. [https://doi.org/10.1016/S0022-1694\(03\)00203-8](https://doi.org/10.1016/S0022-1694(03)00203-8)
- 896 Korus, J. T., Fraundorfer, W. P., Gilmore, T. E., & Karnik, K. (2020). Transient streambed
897 hydraulic conductivity in channel and bar environments, Loup River, Nebraska.
898 *Hydrological Processes*, 34(14), 3061–3077. <https://doi.org/10.1002/hyp.13777>
- 899 Korus, J. T., Gilmore, T. E., Waszgis, M. M., & Mittelstet, A. R. (2018). Unit-bar migration and
900 bar-trough deposition: impacts on hydraulic conductivity and grain size heterogeneity in
901 a sandy streambed. *Hydrogeology Journal*, 26(2), 553–564.
902 <https://doi.org/10.1007/s10040-017-1661-6>
- 903 Kouba, C., & Harter, T. (2024). Seasonal prediction of end-of-dry-season watershed behavior in
904 a highly interconnected alluvial watershed in northern California. *Hydrology and Earth*
905 *System Sciences*, 28(3), 691–718. <https://doi.org/10.5194/hess-28-691-2024>
- 906 Kratzert, F., Nearing, G., Addor, N., Erickson, T., Gauch, M., Gilon, O., Gudmundsson, L.,
907 Hassidim, A., Klotz, D., Nevo, S., Shalev, G., & Matias, Y. (2022). Caravan - A global
908 community dataset for large-sample hydrology. Retrieved from
909 <https://eartharxiv.org/repository/view/3345/>
- 910 Kratzert, F., Klotz, D., Herrnegger, M., Sampson, A. K., Hochreiter, S., & Nearing, G. S. (2019).
911 Toward Improved Predictions in Ungauged Basins: Exploiting the Power of Machine

- 912 Learning. *Water Resources Research*, 55(12), 11344–11354.
913 <https://doi.org/10.1029/2019WR026065>
- 914 Lapides, D., Maitland, B. M., Zipper, S. C., Latzka, A. W., Pruitt, A., & Greve, R. (2022).
915 Advancing environmental flows approaches to streamflow depletion management.
916 *Journal of Hydrology*, 127447. <https://doi.org/10.1016/j.jhydrol.2022.127447>
- 917 Leahy, T. (2016). Desperate Times Call for Sensible Measures: The Making of the California
918 Sustainable Groundwater Management Act. *Golden Gate University Environmental Law*
919 *Journal*, 9(1), 5.
- 920 Li, Q., Zipper, S. C., & Gleeson, T. (2020). Streamflow depletion from groundwater pumping in
921 contrasting hydrogeological landscapes: Evaluation and sensitivity of a new management
922 tool. *Journal of Hydrology*, 590, 125568. <https://doi.org/10.1016/j.jhydrol.2020.125568>
- 923 Li, Q., Gleeson, T., Zipper, S. C., & Kerr, B. (2022). Too Many Streams and Not Enough Time
924 or Money? Analytical Depletion Functions for Streamflow Depletion Estimates.
925 *Groundwater*, 60(1), 145–155. <https://doi.org/10.1111/gwat.13124>
- 926 Mack, S. (1958). *Geology and ground-water features of Scott Valley, Siskiyou County,*
927 *California* (No. Water Supply Paper 1462). *Water Supply Paper* (p. 98). U.S. Govt. Print.
928 Off., <https://doi.org/10.3133/wsp1462>
- 929 Malama, B., Lin, Y.-F., & Kuhlman, K. L. (2024). Semi-Analytical Modeling of Transient
930 Stream Drawdown and Depletion in Response to Aquifer Pumping. *Groundwater*, 62(6),
931 904–919. <https://doi.org/10.1111/gwat.13425>
- 932 Maxwell, R. M., Condon, L. E., & Kollet, S. J. (2015). A high-resolution simulation of
933 groundwater and surface water over most of the continental US with the integrated
934 hydrologic model ParFlow v3. *Geoscientific Model Development*, 8(3), 923–937.
935 <https://doi.org/10.5194/gmd-8-923-2015>
- 936 Messenger, M. L., Lehner, B., Cockburn, C., Lamouroux, N., Pella, H., Snelder, T., Tockner, K.,
937 Trautmann, T., Watt, C., & Datry, T. (2021). Global prevalence of non-perennial rivers
938 and streams. *Nature*, 594(7863), 391–397. <https://doi.org/10.1038/s41586-021-03565-5>
- 939 Mihret, T. T., Zemale, F. A., Worqlul, A. W., Ayalew, A. D., & Fohrer, N. (2025). Unlocking
940 watershed mysteries: Innovative regionalization of hydrological model parameters in
941 data-scarce regions. *Journal of Hydrology: Regional Studies*, 57, 102163.
942 <https://doi.org/10.1016/j.ejrh.2024.102163>
- 943 Nyholm, T., Christensen, S., & Rasmussen, K. R. (2002). Flow Depletion in a Small Stream
944 Caused by Ground Water Abstraction from Wells. *Ground Water*, 40(4), 425–437.
945 <https://doi.org/10.1111/j.1745-6584.2002.tb02521.x>
- 946 Owen, D., Cantor, A., Nylén, N. G., Harter, T., & Kiparsky, M. (2019). California groundwater
947 management, science-policy interfaces, and the legacies of artificial legal distinctions.
948 *Environmental Research Letters*, 14(4), 045016. [https://doi.org/10.1088/1748-](https://doi.org/10.1088/1748-9326/ab0751)
949 [9326/ab0751](https://doi.org/10.1088/1748-9326/ab0751)
- 950 Price, A. N., Zimmer, M. A., Bergstrom, A., Burgin, A. J., Seybold, E. C., Krabbenhoft, C. A.,
951 Zipper, S., Busch, M. H., Dodds, W. K., Walters, A., Rogosch, J. S., Stubbington, R.,
952 Walker, R. H., Stegen, J. C., Datry, T., Messenger, M., Olden, J., Godsey, S. E., ... Ward,
953 A. (2024). Biogeochemical and community ecology responses to the wetting of non-
954 perennial streams. *Nature Water*, 2(9), 815–826. [https://doi.org/10.1038/s44221-024-](https://doi.org/10.1038/s44221-024-00298-3)
955 [00298-3](https://doi.org/10.1038/s44221-024-00298-3)
- 956 Price, A. N., Jones, C. N., Hammond, J. C., Zimmer, M. A., & Zipper, S. C. (2021). The Drying
957 Regimes of Non-Perennial Rivers and Streams. *Geophysical Research Letters*, 48(14),

958 e2021GL093298. <https://doi.org/10.1029/2021GL093298>

959 Reeves, H. W., Hamilton, D. A., Seelbach, P. W., & Asher, A. J. (2009). *Ground-water-*
960 *withdrawal component of the Michigan water-withdrawal screening tool* (Scientific
961 Investigations Report No. 2009–5003) (p. 36). Reston VA: U.S. Geological Survey.
962 Retrieved from <https://pubs.usgs.gov/sir/2009/5003/>

963 Regan, R. S., Juracek, K. E., Hay, L. E., Markstrom, S. L., Viger, R. J., Driscoll, J. M.,
964 LaFontaine, J. H., & Norton, P. A. (2019). The U. S. Geological Survey National
965 Hydrologic Model infrastructure: Rationale, description, and application of a watershed-
966 scale model for the conterminous United States. *Environmental Modelling & Software*,
967 *111*, 192–203. <https://doi.org/10.1016/j.envsoft.2018.09.023>

968 Rohde, M. M., Froend, R., & Howard, J. (2017). A Global Synthesis of Managing Groundwater
969 Dependent Ecosystems Under Sustainable Groundwater Policy. *Groundwater*, *55*(3),
970 293–301. <https://doi.org/10.1111/gwat.12511>

971 Ross, A. (2018). Speeding the transition towards integrated groundwater and surface water
972 management in Australia. *Journal of Hydrology*, *567*, e1–e10.
973 <https://doi.org/10.1016/j.jhydrol.2017.01.037>

974 RRCA. (2003). *Republican River Compact Administration Ground Water Model*. Republican
975 River Compact Administration. Retrieved from <http://www.republicanrivercompact.org/>

976 Sauquet, E., Shanafield, M., Hammond, J., Sefton, C., Leigh, C., & Datry, T. (2021).
977 Classification and trends in intermittent river flow regimes in Australia, northwestern
978 Europe and USA: a global perspective. *Journal of Hydrology*, 126170.
979 <https://doi.org/10.1016/j.jhydrol.2021.126170>

980 Shanafield, M., Bourke, S. A., Zimmer, M. A., & Costigan, K. H. (2021). An overview of the
981 hydrology of non-perennial rivers and streams. *WIREs Water*, *8*(2), e1504.
982 <https://doi.org/10.1002/wat2.1504>

983 Siskiyou County Water Conservation and Flood Control District. (2021). *Scott Valley*
984 *Groundwater Sustainability Plan*. Retrieved from
985 <https://www.co.siskiyou.ca.us/naturalresources/page/scott-valley-final-gsp>

986 Tolley, D., Foglia, L., & Harter, T. (2019). Sensitivity Analysis and Calibration of an Integrated
987 Hydrologic Model in an Irrigated Agricultural Basin With a Groundwater-Dependent
988 Ecosystem. *Water Resources Research*, *55*(9), 7876–7901.
989 <https://doi.org/10.1029/2018WR024209>

990 Towler, E., Foks, S. S., Dugger, A. L., Dickinson, J. E., Essaid, H. I., Gochis, D., Viger, R. J., &
991 Zhang, Y. (2023). Benchmarking high-resolution hydrologic model performance of long-
992 term retrospective streamflow simulations in the contiguous United States. *Hydrology*
993 *and Earth System Sciences*, *27*(9), 1809–1825. [https://doi.org/10.5194/hess-27-1809-](https://doi.org/10.5194/hess-27-1809-2023)
994 [2023](https://doi.org/10.5194/hess-27-1809-2023)

995 Trambly, Y., Rutkowska, A., Sauquet, E., Sefton, C., Laaha, G., Osuch, M., Albuquerque, T.,
996 Alves, M. H., Banasik, K., Beaufort, A., Brocca, L., Camici, S., Csabai, Z., Dakhlaoui,
997 H., DeGirolamo, A. M., Dörflinger, G., Gallart, F., Gauster, T., ... Datry, T. (2021).
998 Trends in flow intermittence for European rivers. *Hydrological Sciences Journal*, *66*(1),
999 37–49. <https://doi.org/10.1080/02626667.2020.1849708>

1000 Vázquez-Suñé, E., Abarca, E., Carrera, J., Capino, B., Gámez, D., Pool, M., Simó, T., Batlle, F.,
1001 Niñerola, J. M., & Ibáñez, X. (2006). Groundwater modelling as a tool for the European
1002 Water Framework Directive (WFD) application: The Llobregat case. *Physics and*
1003 *Chemistry of the Earth, Parts A/B/C*, *31*(17), 1015–1029.

1004 <https://doi.org/10.1016/j.pce.2006.07.008>

1005 White, J. T., Foster, L. K., & Fienen, M. N. (2021). Extending the Capture Map Concept to
 1006 Estimate Discrete and Risk-Based Streamflow Depletion Potential. *Groundwater*, 59(4),
 1007 571–580. <https://doi.org/10.1111/gwat.13080>

1008 Winter, T. C., Harvey, J. W., Franke, O. L., & Alley, W. M. (1998). *Ground water and surface*
 1009 *water: a single resource*. U.S. Geological Survey.

1010 Zimmerman, J. K. H., Carlisle, D. M., May, J. T., Klausmeyer, K. R., Grantham, T. E., Brown,
 1011 L. R., & Howard, J. K. (2018). Patterns and magnitude of flow alteration in California,
 1012 USA. *Freshwater Biology*. <https://doi.org/10.1111/fwb.13058>

1013 Zipper, S. C. (2023). streamDepletr: Estimate Streamflow Depletion Due to Groundwater
 1014 Pumping (Version R package version 0.2.0). Retrieved from [https://CRAN.R-](https://CRAN.R-project.org/package=streamDepletr)
 1015 [project.org/package=streamDepletr](https://CRAN.R-project.org/package=streamDepletr)

1016 Zipper, S. C., Hammond, J. C., Shanafield, M., Zimmer, M., Detry, T., Jones, C. N., Kaiser, K.
 1017 E., Godsey, S. E., Burrows, R. M., Blaszcak, J. R., Busch, M. H., Price, A. N., Boersma,
 1018 K. S., Ward, A. S., Costigan, K., Allen, G. H., Krabbenhoft, C. A., Dodds, W. K., ...
 1019 Allen, D. C. (2021a). Pervasive changes in stream intermittency across the United States.
 1020 *Environmental Research Letters*, 16(8), 084033. [https://doi.org/10.1088/1748-](https://doi.org/10.1088/1748-9326/ac14ec)
 1021 [9326/ac14ec](https://doi.org/10.1088/1748-9326/ac14ec)

1022 Zipper, S. C., Farmer, W. H., Brookfield, A., Ajami, H., Reeves, H. W., Wardropper, C.,
 1023 Hammond, J. C., Gleeson, T., & Deines, J. M. (2022a). Quantifying Streamflow
 1024 Depletion from Groundwater Pumping: A Practical Review of Past and Emerging
 1025 Approaches for Water Management. *JAWRA Journal of the American Water Resources*
 1026 *Association*, 58(2), 289–312. <https://doi.org/10.1111/1752-1688.12998>

1027 Zipper, S. C., Dallemagne, T., Gleeson, T., Boerman, T. C., & Hartmann, A. (2018).
 1028 Groundwater pumping impacts on real stream networks: Testing the performance of
 1029 simple management tools. *Water Resources Research*, 54(8), 5471–5486.
 1030 <https://doi.org/10.1029/2018WR022707>

1031 Zipper, S. C., Gleeson, T., Li, Q., & Kerr, B. (2021b). Comparing Streamflow Depletion
 1032 Estimation Approaches in a Heavily Stressed, Conjunctively Managed Aquifer. *Water*
 1033 *Resources Research*, 57(2), e2020WR027591. <https://doi.org/10.1029/2020WR027591>

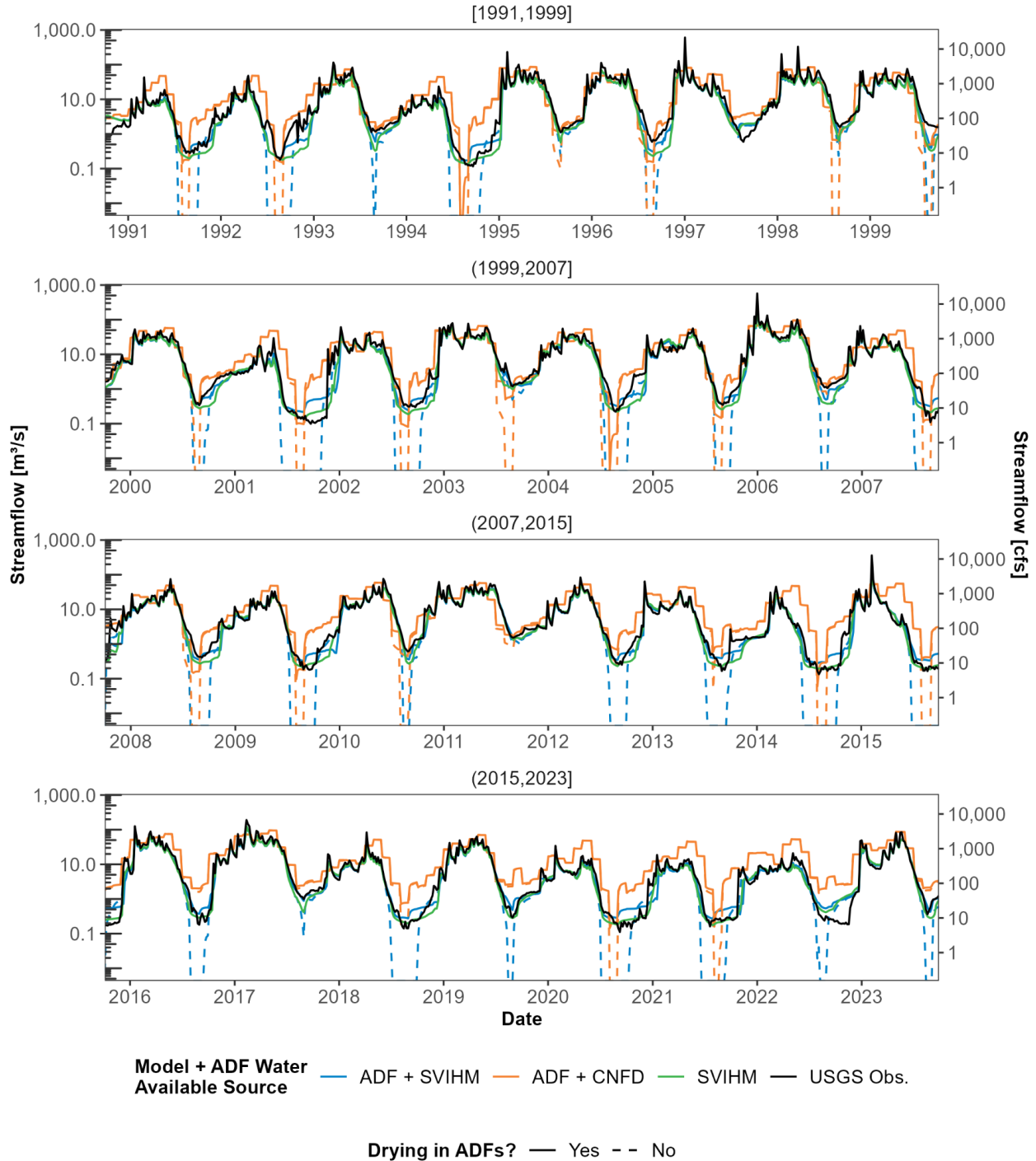
1034 Zipper, S. C., Gleeson, T., Kerr, B., Howard, J. K., Rohde, M. M., Carah, J., & Zimmerman, J.
 1035 (2019). Rapid and Accurate Estimates of Streamflow Depletion Caused by Groundwater
 1036 Pumping Using Analytical Depletion Functions. *Water Resources Research*, 55(7), 5807–
 1037 5829. <https://doi.org/10.1029/2018WR024403>

1038 Zipper, S., Popescu, I., Compare, K., Zhang, C., & Seybold, E. C. (2022b). Alternative stable
 1039 states and hydrological regime shifts in a large intermittent river. *Environmental*
 1040 *Research Letters*, 17, 074005. <https://doi.org/10.1088/1748-9326/ac7539>

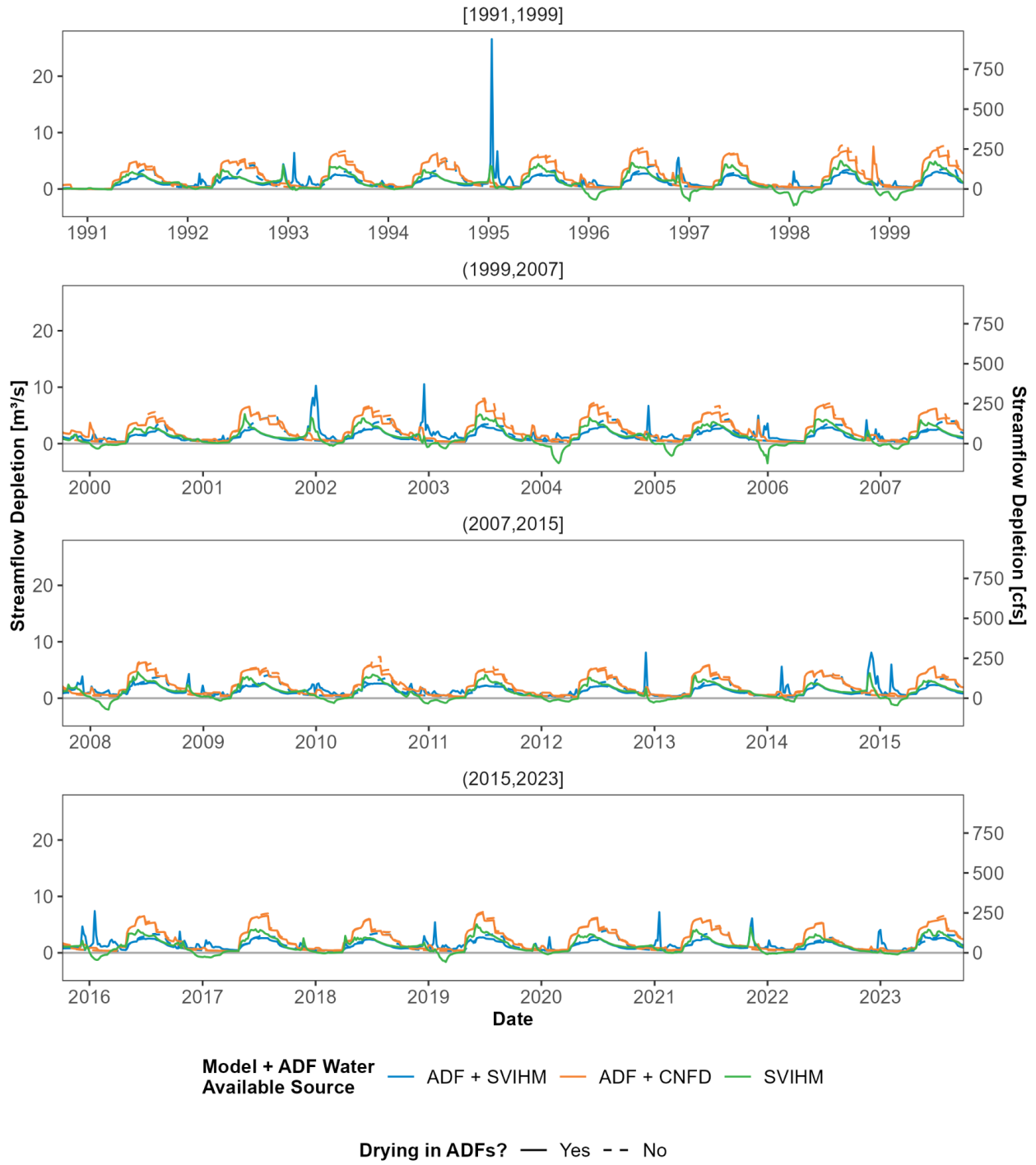
1041 Zipper, S., Brookfield, A., Ajami, H., Ayers, J. R., Beightel, C., Fienen, M. N., Gleeson, T.,
 1042 Hammond, J., Hill, M., Kendall, A. D., Kerr, B., Lapides, D., Porter, M.,
 1043 Parimalarenganayaki, S., Rohde, M. M., & Wardropper, C. (2024). Streamflow Depletion
 1044 Caused by Groundwater Pumping: Fundamental Research Priorities for Management-
 1045 Relevant Science. *Water Resources Research*, 60(5), e2023WR035727.
 1046 <https://doi.org/10.1029/2023WR035727>

1047

1048 Supplemental Information for “Lagged impacts of groundwater pumping on streamflow
 1049 due to stream drying: Incorporation into analytical streamflow depletion estimation
 1050 methods” by Zipper et al.
 1051

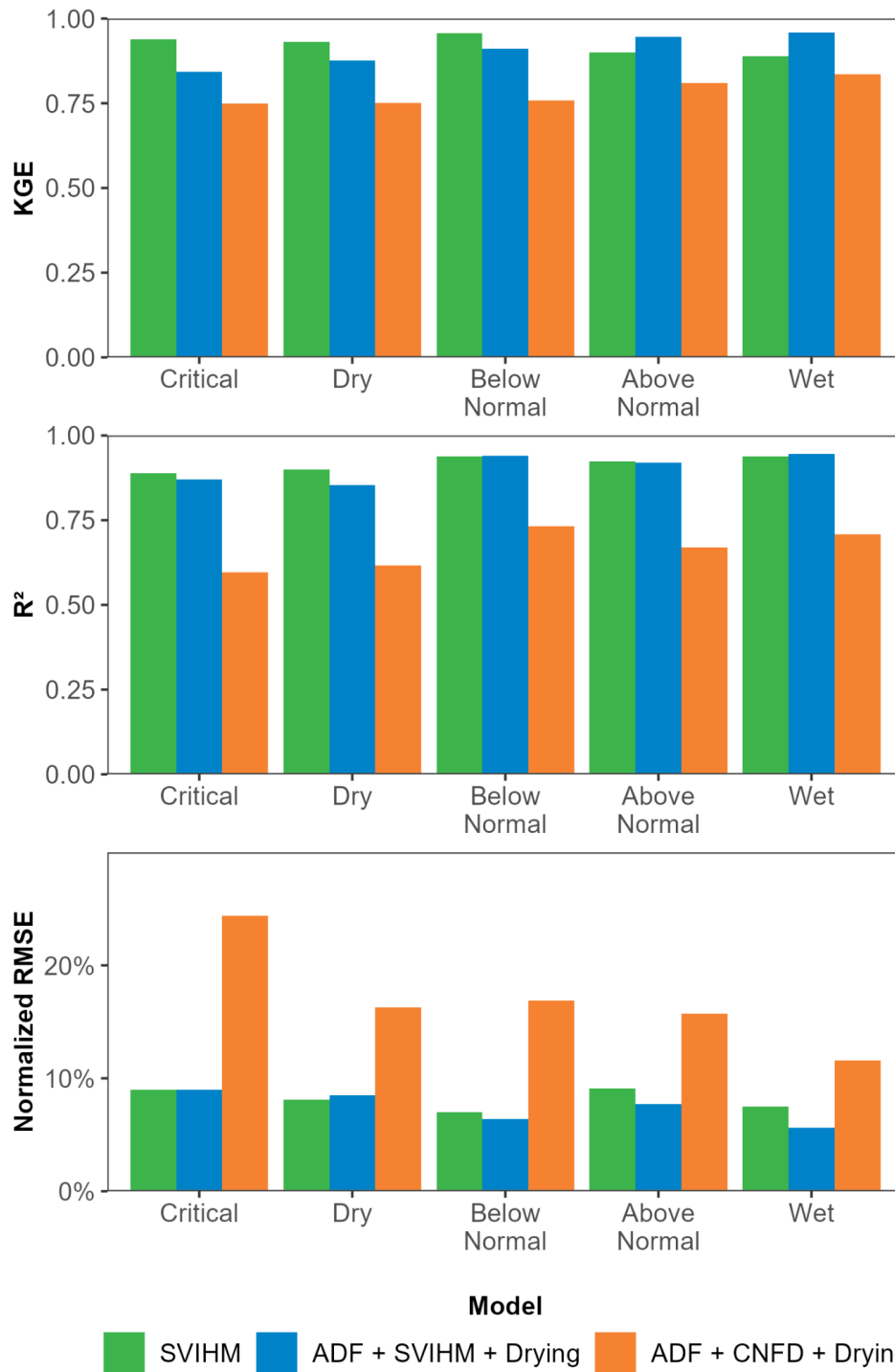


1052
 1053 Figure S1. Streamflow comparison among ADFs, SVIHM, and observations at the watershed outlet for the 33 year
 1054 study period.
 1055



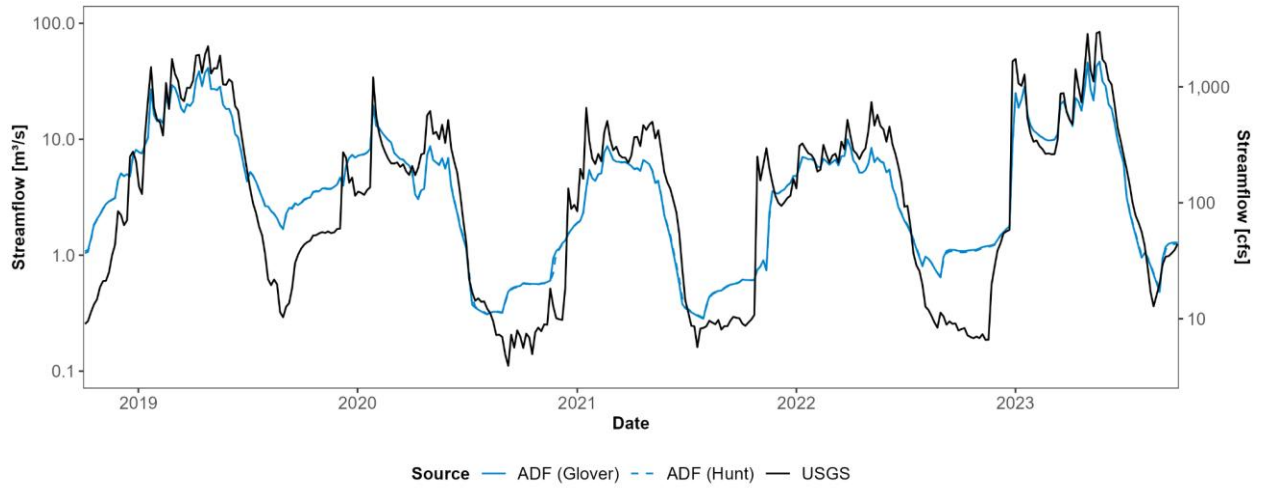
1056
 1057
 1058
 1059

Figure S2. Streamflow depletion comparison between ADFs and SVIHM at the watershed outlet for the 33 year study period.



1060
 1061
 1062
 1063
 1064

Figure S3. Model fit metrics by water year classification. Metrics are calculated via comparison to USGS gauge for log(Streamflow). ADF models include drying. Normalized RMSE is the RMSE divided by the range of observed values.



1065

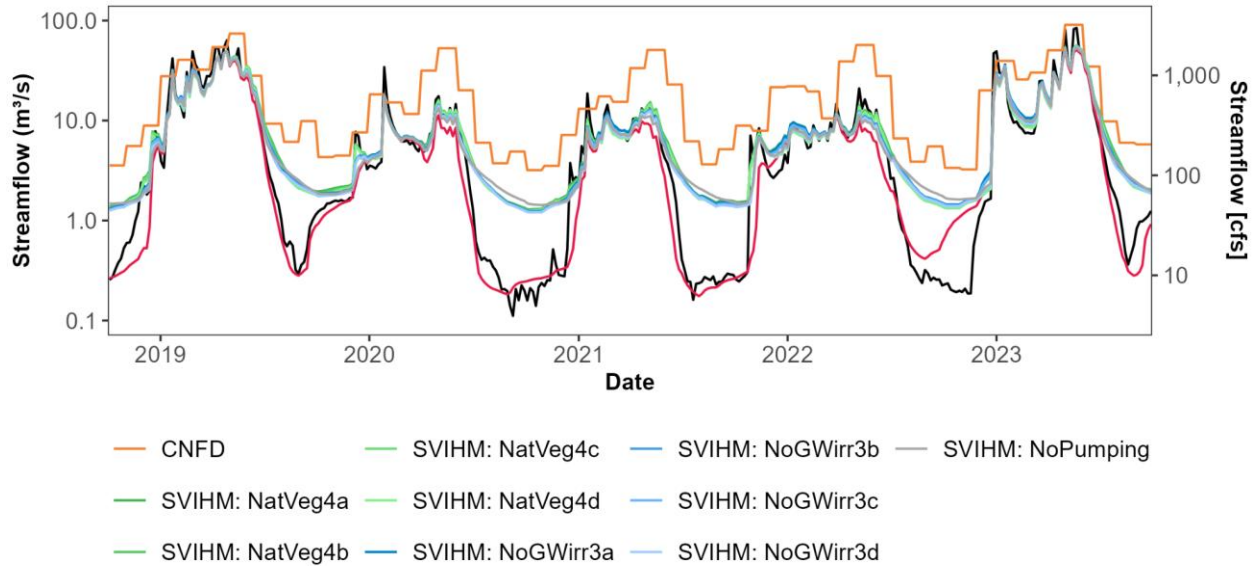
1066 Figure S4. Evaluation of sensitivity of model to choice of analytical solution used in ADFs. The Glover and Hunt
 1067 models produce near-identical results, so the solid and dashed blue lines overlie each other. This indicates that
 1068 streambed conductance is not a limiting factor on streamflow depletion in this domain. All other figures in the
 1069 manuscript use the Hunt model results.

1070

1071 Table S1. Summary of SVIHM model scenarios used in analysis. Scenarios 1 (Basecase) and 3b (No GW Irr Fields)
 1072 are used in the main text.
 1073

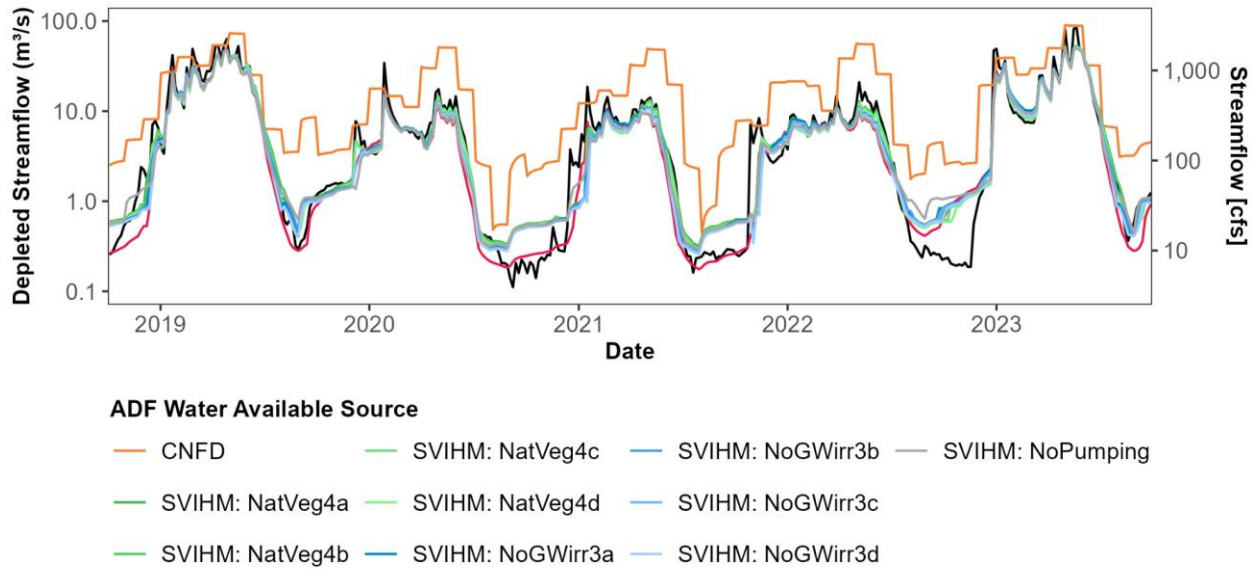
ID	Scenario	Land cover or water source changes	SWBM natVeg root depth	natVeg kc for SWBM	natVeg MODFLOW extinction depth	Interpretation of difference from basecase	
1	Basecase	Basecase land cover.	Basecase (2.4 m)	Basecase (0.6)	Basecase (0 m; 0.5 m in the Discharge Zone)	N/A	
2	No Pumping	Basecase land cover. Water source changes: GW-only → Dry Farming; mixed-GW-SW → SW only				Direct pumping effects, neglecting other land cover-driven changes in water balance. This is not a realistic possibility for real-world, but isolates pumping signal.	
3A	No GW-Irrigated Fields	Assign NatVeg land cover to all GW and Mixed-GW-SW fields	1.2m	0.6	3.05 m	Direct pumping effects + difference in water balance due to natural veg replacing ag in GW irrigated fields	
3B			2.4m	0.6			
3C			1.2m	1.0			
3D			2.4m	1.0			
4A	Native Vegetation (unimpaired flow)	Assign NatVeg land cover to all cultivated fields	1.2m	0.6		3.05 m	Combined effect of all human modifications
4B			2.4m	0.6			
4C			1.2m	1.0			
4D			2.4m	1.0			

1074



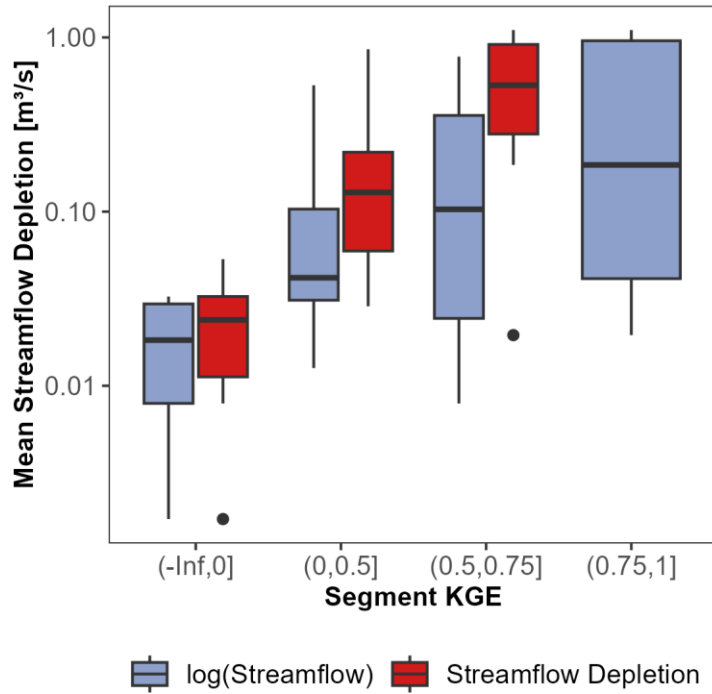
1075

1076 Figure S5. Comparison of streamflow at watershed outlet. The black line shows observed streamflow (source:
 1077 USGS) and the red line shows the SVIHM basecase (pumped) scenario. The colored lines included in the legend
 1078 include CNFD unimpaired flows and nine different SVIHM model configurations. The “basecase” (red) and
 1079 “NoGWirr3b” (blue) scenarios are the basis for results shown in the main text. The other scenarios are meant to
 1080 show sensitivity to vegetation parameterization, which is described in Table S1.
 1081



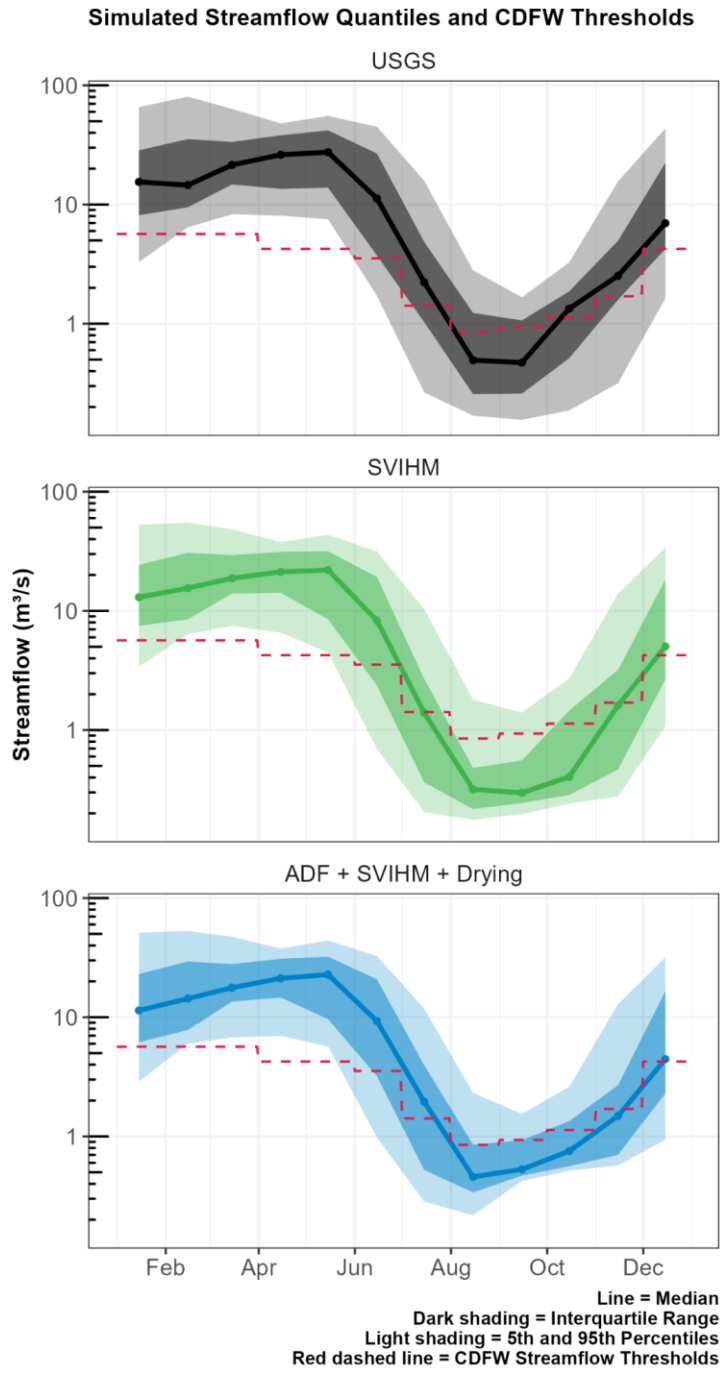
1082
 1083
 1084
 1085
 1086
 1087
 1088
 1089
 1090

Figure S6. Comparison of depleted streamflow at watershed outlet based on ADF simulations using different water available data sources. The black line shows observed streamflow (source: USGS) and the red line shows the SVIHM simulated basecase (pumped) scenario. The colored lines show ADF predicted depleted streamflow using CNFD unimpaired flows and nine different SVIHM model configurations as the water available. ADF models on this plot include drying. The “basecase” (red) and “NoGWirr3b” (blue) scenarios are the basis for results shown in the main text. The other scenarios are meant to show sensitivity to vegetation parameterization, which is described in Table S1.



1091
 1092
 1093
 1094
 1095
 1096

Figure S7. Segment-resolution agreement between ADFs and SVIHM as a function of segment mean streamflow depletion (from SVIHM) in each segment. These results show the ADF + SVIHM + Drying model configuration with water available and SVIHM streamflow depletion calculated using the the SVIHM no-pumping scenario (#2 in Table S1).



1097

1098 Figure S8. Streamflow drought thresholds (red dashed lined) and long-term median, interquartile range, and 5th-95th
 1099 percentile range for streamflow from the USGS observations, SVIHM, and ADF + SVIHM + Drying models.

1100